

PROJECT SUMMARY

Random Matrix Theory for Homogenization of Composites

Overview: In homogenization theory the fundamental challenge is *linkage of scales*. For example, the microstructure of a two phase or polycrystalline composite determines its macroscopic behavior, such as the effective conductivity, as observed on scales much larger than the microstructural scale. Similarly, on large space and time scales, the advection-enhanced effective diffusivity of a tracer in a flowing fluid is determined by the microstructure of the fluid velocity field. A powerful approach to these homogenization problems is the *analytic continuation method*, which provides Stieltjes integral representations for the effective parameters. Information about the *microgeometry* is incorporated through the spectral measure of a self-adjoint random operator which governs classical transport in these complex media and depends only on the microstructure. Indeed, this operator links the microscale to the macroscale. For finite discrete models of these media such as the random resistor network, the operator is a random matrix. The spectral measure, and thus the macroscopic behavior, can be computed in terms of its eigenvalues and eigenvectors.

Consider a composite with electrically conducting and insulating phases. Recently we found that as long range order or connectedness develops with increasing volume fraction of the conducting phase, the eigenvalue statistics, such as the eigenvalue spacing distribution, transition from weakly correlated Poisson-like statistics toward universal Wigner-Dyson (WD) statistics with strong level repulsion. The eigenvectors shift from localized to extended, causing the electric field to spread throughout the system and *mobility edges* to appear. This behavior is strikingly similar to the Anderson transition in quantum, optical, and acoustic systems. However, our findings for classical transport in two phase media are governed by an elliptic equation with random coefficients, where there are *no* interference or scattering effects that are essential to the Anderson transition in wave physics. Here we propose to explore the rich landscape opened up by these unexpected findings at the interface of theories of homogenization for composites, percolation, condensed matter, localization phenomena, and random matrices, including the following issues:

- Since the behavior of the spectral measure controls the critical exponents of transport coefficients near the percolation threshold, are their universal features related to the universal spectral statistics we observe? Is conformal invariance involved in two dimensions?
- How are the geometrical properties of the microstructures related to spectral statistics for the polycrystalline and advection-diffusion problems? Is there an Anderson transition there?
- Develop rigorous analysis of the two phase problem in illustrative cases: dilute limit and Poissonian spectral statistics; quasiperiodic media; etc.
- Investigate *trajectory statistics* for measures on a torus in the polydisc integral representation for effective transport coefficients of three phase composites as one phase percolates.
- Explore the implications of the Anderson-like transition in composites to the analysis of important examples such as multiscale sea ice structures in the climate system, and the optical properties of metal films and suspensions of metal particles in a dielectric host.

Intellectual Merit: We propose to investigate the spectral theory of homogenization for transport in composite media through the lens of random matrix theory, in research which will tie together previously unrelated fields and open up new avenues for investigation and application.

Broader Impacts: Given the highly interdisciplinary nature of the proposed work, we expect impact on our understanding of composite materials and advection diffusion processes in a broad range of application areas. The universality we examine here is shared by many unrelated problems and may provide impacts far beyond theories of composites and inhomogeneous media. The PI Golden has had extensive interactions with the media, and gives many public lectures, so that the results of this research will likely be widely distributed to the public, beyond usual academic channels.

PROJECT DESCRIPTION

Results from Prior NSF Support

AWARD: NSF Grant DMS-0940249, Collaborative Research: *Mathematics and Climate Change Research Network*, 10/01/2010 – 09/30/2016, including a one year no-cost extension.

Total Support across the 12 hub network: \$5,000,000 (\$1,719K to UNC, \$528K to U. Utah, etc.)

PI's: Chris Jones (UNC, Chapel Hill); David Camp (Cal Poly, San Luis Obispo), Chris Danforth (U. Vermont), Inez Fung (UC Berkeley), Kenneth Golden (U. Utah), David Holland (NYU), Eric Kostelich (Arizona State U.), Richard McGehee (U. Minnesota), Ray Pierrehumbert (U. Chicago), Mary Silber (Northwestern), K. K. Tung (U. Washington), and Mary Lou Zeeman (Bowdoin).

Publications resulting from these 12 NSF awards: 181.

Intellectual Merit: The investigators formed a “Mathematics and Climate Research Network” (MCRN) aimed at bringing to bear the full power of modern applied mathematics and statistics on the prediction and understanding of Earth’s climate. We focused on (1) dynamics of climate, (2) climate process modeling, and (3) data analysis and data assimilation. This project is driven by the need to better understand the Earth’s climate system. Climate is the result of many geophysical and chemical processes in the Earth’s land, atmosphere, oceans, cryosphere, and biosphere. These processes evolve in time over many scales, ranging from minutes to centuries, they involve structures on many length scales, ranging from microns to thousands of kilometers, and interact in multiple ways, most often nonlinearly. Feedback mechanisms, many of which are poorly understood, further complicate the picture. Because of the challenges of systematically experimenting on Earth’s climate, the main approach available to climate researchers is through computational experiments. These experiments are based on mathematical models, which must be simple enough not to exceed the capabilities of today’s advanced computer architectures, while still incorporating the physical processes that are essential for realistic climate outcomes. The expertise of mathematical scientists in designing, assessing and interpreting these models is critical. The MCRN helps engage the mathematical sciences community to address the mathematical and statistical issues of our changing climate, helps establish an emerging field of *climate math*, and provides substantial resources to bring young mathematical scientists into the field. Fundamental advances were made in explaining the apparent “pause” in global warming, historical climate events, the evolution of melt ponds on Arctic sea ice, permafrost lakes and methane release, desertification, etc.

Arctic Melt Ponds. In our research program at the University of Utah (partially funded by this grant), we have focused on the challenge of treating multiscale sea ice problems with methods from composite materials and statistical physics. This grant has also partially supported polar expeditions to measure sea ice properties connected to our theoretical modeling research. One of our principal studies has concerned the evolution of the geometrical structure of Arctic melt ponds. During the Arctic melt season, the sea ice surface undergoes a remarkable transformation from vast expanses of snow covered ice to complex mosaics of ice and melt ponds. Sea ice albedo, a key parameter in climate modeling [46, 127, 113, 117], is determined by the complex evolution of melt pond configurations. In fact, ice-albedo feedback has played a major role in the recent declines of the summer Arctic sea ice pack [114]. However, understanding melt pond evolution remains a significant challenge to improving climate projections [46]. By analyzing area–perimeter data from hundreds of thousands of melt ponds, we found an unexpected separation of scales, where the fractal dimension of the pond boundaries transitions from 1 to about 2 around a critical length scale of 100 square meters in area [75]. Pond complexity increases through the transition as smaller ponds coalesce to form large, self-similar connected regions, whose boundaries resemble space filling curves [122]. These features of melt pond evolution are similar to phase transitions in statistical physics [30, 147, 33]. The results impact sea ice albedo, transmitted radiation fields under melting sea ice [48], the heat balance of sea ice and the upper ocean, and biological productivity such as under ice phytoplankton blooms.

We have developed a number of models of melt pond evolution to help understand the observed transition in fractal dimension, as well as other observed geometrical characteristics of melt ponds. First, we have constructed a computationally simple model of melt pond boundaries as the intersection of a horizontal plane, representing the water level, with a random surface representing the topography [19]. We show that an autoregressive class of anisotropic random Fourier surfaces provides topographies that yield the observed fractal dimension transition. We have also introduced a version of the two dimensional Ising model

[30, 147] to describe melt pond evolution, based on the underlying thermodynamics. The model is similar in spirit to the random field Ising model at zero temperature, where the binary spin variables correspond to the presence of melt water or ice on the sea ice surface. With only a minimal set of physical parameters in the model, the predicted pond characteristics evolve from a purely random initial state to agree very closely with observations on the fractal transition as well as power law scaling for the pond size distribution [91]. With two high school students we are close to completing a large project on finding the percolation threshold for melt ponds, and the correlation length exponent for as the threshold is approached. In [145] we have investigated the impact of melt ponds on a low order climate model, and found that the fractal transition can lead to multiple equilibria, bifurcations, and interesting dynamics. The transition of pond configurations from isolated structures to complex interconnected networks is critical in allowing the lateral flow of melt water toward drainage features such as large brine channels, fractures, and seal holes, which can alter the albedo by removing the melt water. We developed algorithmic image processing techniques for mapping photographic images of melt ponds onto conductance networks representing the geometry and connectedness of pond configurations [10]. The effective conductivity is computed to approximate lateral flow.

In May and June of 2014 the MCRN grant partially supported the PI's participation in the NSF Study of Under-Ice Blooms in the Chukchi Ecosystem (SUBICE), to study melt pond formation on Arctic sea ice and associated under-ice algal blooms. The initial formation of ponds requires that melt water be retained above sea level on the ice surface. Both theory and observations, however, show that first year sea ice is so highly porous prior to the formation of melt ponds that multi-day retention of water above hydraulic equilibrium should not be possible. In [116] we present results of percolation experiments that identify and directly demonstrate the mechanism allowing melt pond formation. The infiltration of fresh water into the pore structure of sea ice is responsible for blocking percolation pathways with ice, sealing the porous microstructure against water percolation, and allowing water to pool above sea level. The blockage process has the potential to exert significant control over inter-annual variability in ice albedo.

Fluid and Electromagnetic Transport in Sea Ice. Another major direction partially funded by the MCRN grant (and an NSF Collaborations in Mathematical Geosciences grant) was aimed at developing the mathematical and electromagnetic methods necessary to remotely monitor the internal state of sea ice, its porous brine microstructure, and fluid and thermal transport through the ice. Such developments help track key transitions in the state of the polar ice packs and improve projections of their fate and impact on ecosystems. Toward these goals we have conducted field experiments on the fluid and electromagnetic transport properties of sea ice in the Arctic in 2011, 2012, 2013, and 2014 and in the Antarctic in 2010 and 2012. Fluid flow through sea ice mediates a broad range of geophysical and biological processes in the polar marine environment. For example, the evolution of melt ponds and summer ice albedo is constrained by drainage through porous sea ice [41]. However, for brine volume fractions below about 5%, columnar sea ice is effectively impermeable to fluid flow, while it is increasingly permeable for volume fractions above 5%. This critical behavior of fluid transport is known as the *rule of fives* [64, 66, 118]. In two different experiments conducted in the Arctic and Antarctic, we have found that this critical threshold for fluid flow exhibits a strong, characteristic electrical signature [65]. Conductivity data are accurately explained by percolation theory, with the same critical exponent that describes fluid permeability [66]. The data also indicate marked changes in the conductivity profile with melt pond onset. Rigorous relations between fluid and electrical transport enable us to partition the resistivity range into intervals corresponding to regimes of permeability characteristics and related processes, such as melt pond development, and fluxes of nutrients and CO₂.

We have constructed a network model of electrical transport in sea ice [158], built on an earlier network model for fluid flow [159], to help explain our experimental results and connect fluid and electrical transport. We developed a rigorous method for recovering microstructural information about sea ice from electromagnetic measurements [109], obtaining the first results on inverting effective complex permittivity data for information about the *connectedness* of inclusions in a composite, and applied these results to sea ice. Moreover, we developed a Stieltjes representation for the effective complex permittivity of polycrystalline composites, found rigorous bounds based on crystallographic information, and applied them to sea ice [73]. We obtained inverse bounds, enabling us to remotely distinguish between columnar and granular crystalline microstructures, which have markedly different fluid transport properties as we found in the Antarctic [67].

Broader Impacts: The MCRN aims to be a national resource, with participants working together as a virtual community over the internet. This effort is defining a research area of *climate mathematics* and educating

a new generation of mathematical researchers with over 100 supported - to meet the scientific challenges associated with a changing climate. Award winning educational materials were produced, and a range of outreach activities were sponsored. During this period, there were over 20 media articles on Golden's research, including profiles in *Scientific American* and *Physics Today*. He was featured in numerous radio and television interviews, and three videos produced by NSF and NBC News. Through these outreach efforts, we have helped publicize the loss of Arctic sea ice, and the role of mathematics in studying climate.

AWARD: NSF Grant DMS-1413454, *Homogenization for Sea Ice*, 8/1/2014 – 7/31/2017.

Total Support: \$320,000

PI: K. M. Golden, co-PIs: E. Cherkaev and C. Strong (Atmospheric Sciences, U. of Utah),

Publications partially supported by this award: 11.

Intellectual Merit: One of the fundamental challenges of climate science is to develop more rigorous representations of sea ice in climate models, and account for important sub-grid scale processes and their projection onto larger scale patterns of change. Sea ice exhibits composite structure over many orders of magnitude: sub-millimeter scale brine inclusions which can coalesce into meter scale channels, melt ponds on scales from centimeters to hundreds of meters, and sea ice floes on centimeter to kilometer scales, which form the “microstructure” of the ice pack. Here the pack is viewed as a composite of ice floes and ocean, or ice floes and a viscous slurry of sea water and much smaller ice crystals and broken bits. In this project we aim to apply methods of homogenization for composites to analyzing effective behavior of sea ice on scales relevant to climate models. We consider several issues where the mathematics of composites can provide a rigorous framework for analysis and computation of sea ice properties.

In the Arctic warm season, the large-scale spatial pattern of sea ice is a central mass of *pack ice* surrounded by a band of broken ice called the marginal ice zone (MIZ), which in turn is surrounded by open ocean. The MIZ can be defined as the region where the sea ice concentration field (or area fraction of ice floes vs. water) ranges from 80% down to 15%. The width of the MIZ is a fundamental length scale for polar physical and biological dynamics. However, measuring this width is not straightforward, given the complex, dynamic nature of the MIZ boundary. By averaging the arc length of the streamlines of a potential (or idealized sea ice concentration field) satisfying Laplace's equation with the above boundary conditions, Strong [141] established an objective method for measuring MIZ width. This method was used to find a 39% widening of the MIZ during 1979-2011 [144]. In [142] we used an eccentric annulus as a simplified model of MIZ geometry to introduce and study relevant definitions of the width. We discovered that the width of the warm-season MIZ has recently collapsed back to its narrowest observed values (ca. 1980). We adapted the use of Laplace's equation as an idealized sea ice concentration field to the problem of filling the “polar data gap,” which is a region around the North Pole where satellite orbit and instrument swath preclude retrieval of sea ice concentrations [143]. Realistic spatial heterogeneity was achieved by adding a spatially autocorrelated stochastic field based on observations, thus providing a computationally simple approach to solving the polar data gap problem. Moreover, this approach based on an elliptic PDE has sufficient generality to provide more sophisticated and accurate models.

In fact, one focus is on generalizing the Laplace analysis to include an inhomogeneous diffusivity in the transport equation, and investigating how this effective coefficient is related to smaller scale information on ice pack microgeometry. We are inverting satellite data for the local coefficient. We have formulated and performed an approximate inversion along streamlines, and extended the analysis to more sophisticated models. We are also looking at the connection of the recovered local diffusivity to the homogenized parameter in a numerical advection diffusion model for ice pack dynamics. In related analytical work, we have developed Stieltjes integral representations for the effective diffusivity of advection diffusion equations with time independent [105] and time dependent [104] flow fields, and begun spectral measures computations.

Recently there has been an increasing realization of the importance of the influence of wave-ice interactions in the MIZ on the growth and decay of the seasonal ice pack. In the important quasistatic regime we have developed a Stieltjes integral representation for the effective complex viscoelastic tensor for ocean wave propagation through the ice-water composite, involving a spectral measure. We have also obtained bounds on this parameter in terms of the ice pack microgeometry.

In other homogenization problems for sea ice, we have built on our previous work on network models for transport in sea ice to examine the effect of entrained exopolymeric substances (EPS) secreted by sea ice algae on effective fluid flow properties [138]. With a high school student we found the thermal conductivity

of sea ice in the presence of convection via an inverse problem [34]. The “best” composite structures which fit thermal data from Antarctica are found.

Finally, a principal direction we have pursued is to develop mathematical techniques for *upscaling* local information about sea ice to obtain effective properties on larger scales. In the analytic continuation method for studying the effective properties of composites [58, 11, 98] (see below), the microstructural characteristics are incorporated into integral representations of the effective properties through a *spectral measure* of a self-adjoint operator which depends only on the composite microgeometry. For a discretized image of any composite structure, the computation of the spectral measure reduces to finding the eigenvalues and eigenvectors of a symmetric random matrix [103]. We have carried out such computations for examples of the brine phase in sea ice, melt ponds on Arctic sea ice, and the ice pack itself [107]. In examining eigenvalue statistics for various microstructures, we discovered that the statistics exhibit striking transitions as connectivity thresholds are approached [102], which is what led to the current proposal.

Broader Impacts: The funds from this award have partially supported the research of two graduate students, two undergraduates, and one high school student. The investigators, particularly the PI, have given many lectures for the general public and been involved in a number of outreach efforts. Please see the previous award for media impact.

AWARD: NSF Award DMS-1615762, *Frontier Probability Days Conference*, 6/1/2016 - 5/31/2017

Total Support: \$25,000

PI: Tom Alberts, Co-PI's Davar Khoshnevisan (University of Utah), Firas Rassoul-Agha (University of Utah), Sunder Sethuraman (University of Arizona), Ed Waymire (Oregon State University).

Publications: No publications were produced under this award.

Intellectual Merit: The conference featured high quality, recent research in disordered systems, random matrices, stochastic processes on Lie groups, and stochastic biology.

Broader Impacts: This conference exposed young researchers to the latest trends in probability theory and its applications, and helped them to establish a network of future collaborators. Funds supported travel expenses for 3 (of 7) plenary speakers and 25 graduate students or postdocs.

1 Introduction

Multiphase or polycrystalline composite materials [99, 148, 13] arise throughout the physical, geophysical, engineering, and biological sciences, and are used in myriad industrial and medical applications. Similarly, diffusive transport in the presence of a flow field [94, 14, 43, 44, 112, 92, 93, 156] is also widely encountered in science and engineering. In these systems we are typically most interested in the effective or *homogenized* behavior on length scales much larger than the scale of local variations of the composite microstructure or flow field. For example, in multiphase or polycrystalline composites, the effective transport coefficients such as electrical or thermal conductivity, complex permittivity, and magnetic permeability determine the bulk behavior of the medium. For problems involving diffusion in a flow field the advection-enhanced effective diffusivity determines the behavior on large space and time scales. The powerful analytic continuation method [12, 98, 58, 99] for addressing the homogenization or *linkage of scales* problem was originally developed for two phase random media. It has been extended to these other cases as well: three or more phases [59, 51], polycrystalline composites [73], and advection diffusion [3, 4, 5, 105, 104].

At the heart of the method are Stieltjes integral representations for the effective parameters, involving spectral measures that incorporate the microstructural geometry of the composite or flow field. The spectral measures come from a bounded self-adjoint linear operator G that depends only on this microstructural geometry. For finite discrete systems like random resistor network models of media in the continuum, this operator is a random matrix, and the spectral measure can be computed from the eigenvalues and eigenvectors of this matrix. By developing the mathematical foundation for these computations [103] and studying the properties of computed spectral measures for a broad range of microstructures [68, 107], we discovered that the statistics of the eigenvalues displayed fascinating behavior depending on the connectedness of one of the phases. While there have been earlier statistical investigations of the “geometric resonances” of binary media [80, 71, 70], the operators and computations were different than ours, and the striking, unexpected picture which emerged in [102] and led to this proposal was not previously revealed.

Random matrix theory (RMT) [72, 16, 95, 37] has been quite successful in modeling universal features

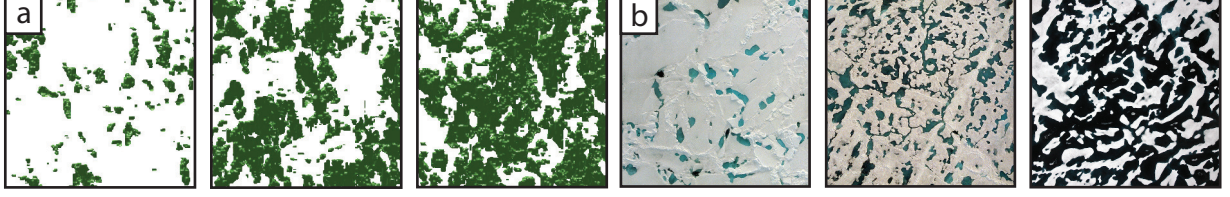


Figure 1: **Connectedness transitions in composites.** Increasingly connected composite structures from left to right (a-b). (a) X-ray CT volume renderings of the brine phase within a lab-grown sea-ice single crystal (H. Eicken), with brine area fractions $\phi = 0.20$, $\phi = 0.51$, and $\phi = 0.70$. (b) Melt ponds on the surface of Arctic sea ice (D. K. Perovich), with area fractions $\phi = 0.09$, $\phi = 0.27$, and $\phi = 0.57$.

found in statistical fluctuations of characteristic quantities of complex systems, such as atomic nuclei [72], biological networks [90], financial time series [115], quantum systems whose classical counterparts are chaotic [87, 72], and mesoscopic conductors [139]. Even the (non-random) zeros of the famous Riemann zeta function have universal features which are accurately captured by RMT [97, 95, 87]. These systems can be described in terms of discrete “spectra” on a line. In RMT, the spectra of such systems are modeled by the eigenvalues of ensembles of random matrices called random matrix ensembles (RME’s), including the Gaussian Orthogonal Ensemble (GOE) and the Gaussian Unitary Ensemble (GUE). Long and short range correlations of these random eigenvalues are measured in terms of various eigenvalue statistics introduced by Dyson and Mehta [95]. The localization properties of the eigenvectors are characterized by quantities such as the inverse participation ratio (IPR) [115] and the Shannon information entropy [96].

In many systems, the spectral statistics are parameter independent when properly scaled [72, 25] and fall into two *universal* categories: uncorrelated Poisson statistics [72] and highly correlated Wigner–Dyson (WD) statistics [72, 37]. The statistical behavior of the spectrum is related to the extent that the eigenfunctions overlap. A key example is the Anderson theory of the metal-insulator transition (MIT) [2, 42], which provides a powerful, quantum mechanical framework for understanding when a disordered medium allows electronic transport, and when it does not. Indeed, for large enough disorder the electrons are localized in different places, with uncorrelated energy levels described by Poisson statistics [133, 86]. For small disorder, the wave functions are extended and overlap, giving rise to correlated Wigner-Dyson (WD) statistics [133, 86] with strong level repulsion [72]. For intermediate disorder hybrid Poisson-like level statistics arise [133, 25]. There are other systems which undergo an analogous spectral transition as a system parameter varies, including the hydrogen atom in a magnetic field [38], random points on a fractal set [125], quantum chaos [130, 129, 155], and complex networks [96, 8, 78, 110, 31].

Consider the effective transport coefficients of macroscopic two phase composites [99, 148, 13]. For example, electrical conduction is described by (a weak form of) $\nabla \cdot (\sigma \nabla \phi) = 0$ with potential ϕ , electric field $E = -\nabla \phi$, and local conductivity σ taking the values σ_1 or σ_2 . A metal–insulator mixture is modeled with $h = \sigma_1/\sigma_2 \rightarrow 0$. Near a percolation threshold the system undergoes a *classical* MIT with the effective conductivity σ^* described by critical exponents [137, 13, 32]. The underlying physics of the quantum and classical MIT are quite different. Anderson localization in quantum systems, described by the Schrödinger equation, is a wave interference phenomenon, which appears to be common to all wave systems, such as in optics [128] and acoustics. On the other hand, for transport in macroscopic two phase media governed by the elliptic equation above, there are *no* wave interference or scattering effects and *no* quantum phenomena.

It is surprising then that the random operator G governing effective transport in composites has spectral properties that transition in a way that is strikingly similar to the Anderson transition in wave mechanics. We find [102] that *phase connectedness* in composites determines the Anderson-like transition in the spectral properties of G . The critical volume fraction at the percolation threshold [137] plays the role of the critical level of disorder necessary for localization in wave physics.

As mentioned above, the operator G arises in the analytic continuation method [12, 98, 58] for studying transport in two phase composites. For finite discrete media the action of G is given by a *random matrix* M and the spectral measure as well as the electric field \mathbf{E} are given *explicitly* in terms of its eigenvalues and eigenvectors [103, 13]. We observe that as the conducting phase percolates, the eigenvectors of G shift from localized to extended, causing the electric field \mathbf{E} to spread throughout the system. Near the

connectedness-driven MIT *mobility edges* appear, analogous to Anderson localization where mobility edges mark the characteristic energies of the quantum MIT [72]. The overlap of eigenvectors of G gives rise to a transition in the statistical properties of the eigenvalues from weakly correlated Poisson-like statistics toward universal Wigner-Dyson (WD) statistics with strong level repulsion [133, 72, 86]. This eigenvalue repulsion explains the collapse of spectral gaps as connectedness develops [106, 80, 35, 103], which is related to critical behavior [13, 32, 7, 60, 106, 80, 35]. The locations of the eigenvalues on the negative real axis in the h -plane correspond to singularities of the transport coefficients [99, 13, 80, 32]. In the context of the optical properties of metallic particles in an insulating host [13], for example, the resonance structure of the effective complex permittivity and the absorption profile, such as sharp peaks associated with *surface plasmon resonances* [13, 49], are observable [13, 32] and determined by the spectral properties of G .

Here we propose to walk through the door opened by our unexpected findings on the Anderson transition for two phase media. We will delve further into that arena with investigation of key examples, like quasiperiodic media, and address a number of theoretical issues, such as the connection of our findings to universality of critical exponents. We will explore this RMT phenomenon in new application areas where the underlying analytic framework carries over: polycrystalline media, advection diffusion, and the several complex variable multicomponent problem. Finally, we will investigate the impacts of our findings on some examples of composites, such as multiscale sea ice structures, and metal-insulator composites.

2 Formulation: Percolation, Composites, and Random Matrices

Percolation models. Consider the d -dimensional integer lattice \mathbb{Z}^d , and the square or cubic network of bonds joining nearest neighbor lattice sites. In the percolation model [20, 137, 69, 22], we assign to each bond a conductivity $\sigma_0 > 0$ with probability p , meaning it is open (black), and with probability $1 - p$ we assign a 0, meaning it is closed. Three examples of lattice configurations are shown in Fig. 2. Groups of connected open bonds are called *open clusters*. In this model there is a critical probability p_c , $0 < p_c < 1$, called the *percolation threshold*, at which the average cluster size diverges and an infinite cluster appears. For the two dimensional bond lattice $p_c = 1/2$. For $p < p_c$ the density of the infinite cluster $P_\infty(p)$ is 0, while for $p > p_c$, $P_\infty(p) > 0$ and near the threshold, $P_\infty(p) \sim (p - p_c)^\beta$ as $p \rightarrow p_c^+$, where β is a universal critical exponent, that is, it depends only on dimension and not on the details of the lattice. Let $x, y \in \mathbb{Z}^d$ and $\tau(x, y)$ be the probability that x and y belong to the same open cluster. Then for $p < p_c$, $\tau(x, y) \sim e^{-|x-y|/\xi(p)}$, and the correlation length $\xi(p) \sim (p_c - p)^{-\nu}$ diverges with a universal critical exponent ν as $p \rightarrow p_c^-$.

The effective conductivity $\sigma^*(p)$ of the lattice, now viewed as a random resistor (or conductor) network, defined via Kirchoff's laws, vanishes for $p < p_c$ like $P_\infty(p)$ since there are no infinite pathways. For $p > p_c$, $\sigma^*(p) > 0$, and near p_c , $\sigma^*(p) \sim \sigma_0(p - p_c)^t$, $p \rightarrow p_c^+$, where t is the conductivity critical exponent, with $1 \leq t \leq 2$ in $d = 2, 3$ [52, 54, 62], and numerical values $t \approx 1.3$ in $d = 2$ and $t \approx 2.0$ in $d = 3$ [137]. Consider a random pipe network with effective fluid permeability $k^*(p)$ exhibiting similar behavior $k^*(p) \sim k_0(p - p_c)^e$, where e is the permeability critical exponent, with $e = t$ [26, 124, 62]. Both t and e are believed to be universal – they depend only on dimension and not the lattice. Continuum models can exhibit nonuniversal behavior with exponents different from the lattice case and $e \neq t$ [74, 45, 137, 123, 83].

Composites, analytic continuation, and spectral measures. We now briefly describe the *analytic continuation method* (ACM) for studying the effective transport properties of composite materials [12, 98, 58, 99, 61]. Later we will show how this method may be adapted to studies of polycrystalline media [73, 9] and advection-enhanced diffusion of passive tracers by incompressible fluid velocity fields [3, 4].

For simplicity, we consider the electrical conductivity tensor σ of a two phase random medium, although the method applies to any classical transport coefficient [99]. Here, $\sigma(x, \omega)$ is a (spatially) stationary random field in $x \in \mathbb{R}^d$ and $\omega \in \Omega$, where Ω is the set of all geometric realizations of the medium, which is indexed by the parameter ω representing one particular realization, and the underlying probability measure P is compatible with stationarity [58]. The field equations [77, 58] are as follows,

$$\nabla \times E = 0, \quad \nabla \cdot J = 0, \quad J = \sigma E, \quad \langle E \rangle = e_k, \quad (1)$$

where $E(x, \omega)$ and $J(x, \omega)$ are stationary electric and current fields, respectively, e_k is a standard basis vector in the k th direction, and $\langle \cdot \rangle$ denotes ensemble averaging over Ω or spatial average over all of \mathbb{R}^d [58].

The effective conductivity tensor σ^* is defined by [58]

$$\langle J \rangle = \sigma^* \langle E \rangle. \quad (2)$$

Later, we will consider a polycrystalline medium where the local conductivity σ is a non-trivial symmetric matrix. Here we consider a two-phase locally isotropic medium, where the components σ_{jk} of σ satisfy $\sigma_{jk}(x, \omega) = \sigma(x, \omega) \delta_{jk}$, where δ_{jk} is the Kronecker delta and

$$\sigma(x, \omega) = \sigma_1 \chi_1(x, \omega) + \sigma_2 \chi_2(x, \omega). \quad (3)$$

Here, σ_j is the value of the conductivity for medium $j = 1, 2$ (which can be complex) and $\chi_j(x, \omega)$ is its characteristic function, equaling 1 for $\omega \in \Omega$ with medium j at x , and 0 otherwise, with $\chi_2 = 1 - \chi_1$. For isotropic media, we focus on one diagonal coefficient $\sigma^* = \sigma_{kk}^*$, with $\sigma^* = \langle \sigma E \cdot e_k \rangle$. By homogeneity of $\sigma(x, \omega)$, σ^* depends on the contrast parameter $h = \sigma_1/\sigma_2$ and we define $m(h) = \sigma^*/\sigma_2$, which is a Herglotz function that maps the upper half h -plane to the upper half plane, and is analytic off $(-\infty, 0]$ [11, 58].

The key step in the method [58, 11, 98, 99] is obtaining a Stieltjes integral representation for σ^* , which follows from a resolvent representation of the electric field (in material phase 1) [58, 103]

$$\chi_1 E = s(sI - G)^{-1} \chi_1 e_k, \quad G = \chi_1 \Gamma \chi_1, \quad (4)$$

where $\Gamma = -\nabla(-\Delta)^{-1}\nabla$ acts as a projection from $L^2(\Omega, P)$ onto the Hilbert space of curl-free random fields [58], and $(-\Delta)^{-1}$ is based on convolution with the free space Green's function for the Laplacian $\Delta = \nabla^2$. Consider the function $F(s) = 1 - m(h)$, $s = 1/(1 - h)$, which is analytic off $[0, 1]$ in the s -plane. Then writing $\sigma = \sigma_2(1 - \chi_1/s)$ in (3) yields [58, 103]

$$F(s) = \langle [(sI - \chi_1 \Gamma \chi_1)^{-1} \chi_1 e_k] \cdot e_k \rangle = \int_0^1 \frac{d\mu(\lambda)}{s - \lambda}, \quad s = \frac{1}{1 - \sigma_1/\sigma_2}, \quad (5)$$

where $\mu(d\lambda) = \langle Q(d\lambda) \chi_1 e_k \cdot e_k \rangle$ is a positive *spectral measure* on $[0, 1]$ and $Q(d\lambda)$ is the projection valued measure uniquely determined by the random, bounded, self-adjoint operator $G = \chi_1 \Gamma \chi_1$ [58, 140].

Equation (5) is based on the spectral theorem [120, 140] for the resolvent of the operator $G = \chi_1 \Gamma \chi_1$. It provides a Stieltjes integral representation for the effective complex conductivity σ^* which separates the component parameters in s from the complicated geometrical information contained in the measure μ . This measure is the same for all classical transport coefficients, spectrally coupling these properties of the composite [27, 28, 29]. Information about the geometry enters through the moments $\mu_n = \int_0^1 \lambda^n d\mu(\lambda) = \langle [(\chi_1 \Gamma \chi_1)^n e_k] \cdot e_k \rangle$, $n = 1, 2, 3, \dots$. For example, the mass μ_0 is given by $\mu_0 = \langle \chi_1 e_k \cdot e_k \rangle = \langle \chi_1 \rangle = \phi$, where ϕ is the volume or area fraction of phase 1, and $\mu_1 = \phi(1 - \phi)/d$ if the material is statistically isotropic [58, 21]. In general, μ_n depends on the $(n + 1)$ -point correlation function of the medium.

In the discrete setting of a square lattice, the action of the operator G is given by that of a real-symmetric random matrix M , where Γ is a (non-random) projection matrix which depends only on the lattice topology and boundary conditions, and χ_1 is a diagonal (random) projection matrix which determines the geometry and component connectivity of the composite medium [103]. In this setting, E and the integral in equations (4) and (5) have explicit representations in terms of the eigenvalues λ_i and eigenvectors u_i of M [103]

$$\chi_1 E = sE_0 \sum_i \frac{\sqrt{m_i}}{s - \lambda_i} u_i, \quad F(s) = \sum_i \frac{m_i}{s - \lambda_i}, \quad m_i = |u_i \cdot \chi_1 \hat{e}_k|^2, \quad (6)$$

where \hat{e}_k plays the role of a standard basis vector on the lattice. This shows the discrete spectral measure μ is given explicitly in terms of the eigenvalues λ_i and orthonormal eigenvectors u_i of the matrix M [103]:

$$\mu(d\lambda) = \langle Q(d\lambda) \hat{e}_k \cdot \hat{e}_k \rangle, \quad Q(d\lambda) = \sum_i \delta_{\lambda_i}(d\lambda) \chi_1 Q_i, \quad Q_i = u_i u_i^T. \quad (7)$$

Here, $Q(d\lambda)$ is the projection valued measure associated with M , $\delta_{\lambda_i}(d\lambda)$ is the delta measure concentrated at λ_i , and $Q_i = u_i u_i^T$ is the projection matrix associated with the eigenspace spanned by u_i [103].

To compute μ a non-standard generalization of the spectral theorem for matrices is required, due to the projective nature of the matrices χ_1 and Γ [103]. In particular, we developed a *projection method* that demonstrates the spectral measure μ in (7) depends only on the eigenvalues and eigenvectors of random sub-matrices of Γ of size $N_1 \approx pN$ corresponding to diagonal components $[\chi_1]_{ii} = 1$ [103]. Moreover for the periodic setting, the matrix Laplacian is singular so the matrix representation of $(-\Delta)^{-1}$ is not defined. We

have recently extended the results in [103] to the periodic setting, utilizing properties of the singular value decomposition (SVD) of the matrix gradient ∇ . This extension not only alleviated the issues associated with the 3D RRN discussed in [103] but also gave rise to new spectral behaviors [102] not previously discovered in related numerical investigations [80, 71, 70], demonstrating that use of periodic boundary conditions provides a more correct representation of an infinite, stationary random medium.

Classical RMT. Classical random matrix theory was initially developed as a way to study the energy levels of electrons in complicated atomic nuclei [154], but has since become ubiquitous in statistics [79, 111, 50], finance [89, 18], wireless communication [152], neuroscience [153, 119], and even number theory [97, 95, 87]. Up to normalization, the classical ensemble of all $N \times N$ random matrices with given symmetries (real-symmetric, Hermitian, etc.) has an eigenvalue distribution $P(\lambda_1, \dots, \lambda_N)$ of the form [108, 37, 139, 95, 25]

$$P(\lambda_1, \dots, \lambda_N) = \prod_{i < j=1}^N |\lambda_i - \lambda_j|^\beta \prod_{i=1}^N \exp[-V(\lambda_i)]. \quad (8)$$

Here, β depends only on the symmetry of the RME and is equal to 1, 2, or 4 for ensembles with orthogonal, unitary, or symplectic symmetries [37]. It is well known that the rescaled empirical measure of the eigenvalues converges to Wigner's famous semicircle law [6, 146], while the unscaled eigenvalues converge to Dyson's Sine process [40, 1]. The extreme eigenvalues converge to the famous Tracy-Widom distribution [149, 150]. It was initially believed that the local eigenvalue statistics of such RME's were independent of the function $V(\lambda)$, and were generically given by WD statistics of eigenvalues [25]. This initial study [95, 25] used a class of functions $V(\lambda)$, known as strong confining potentials, which is characterized by power-law asymptotic growth $V(\lambda) \sim |\lambda|^\alpha$, $\alpha > 0$, as $|\lambda| \rightarrow \infty$. This universal behavior has been rigorously proven for a large class of strong confining potentials [36, 37] and supported by numerical evidence [25].

However, during a study of the Anderson transition, it was inferred [108, 139] that there is another class of functions $V(\lambda)$, known as weak confining potentials, for which the eigenvalue statistics deviate from the universal WD behavior toward Poisson statistics. This class of functions is characterized by a very slow asymptotic growth $V(\lambda) \sim A \ln^2 |\lambda|$, as $|\lambda| \rightarrow \infty$. As the positive parameter A decreases from one, the eigenvalue statistics transition from WD-like statistics toward Poisson statistics [25].

For unitary RME's with $\beta = 2$, this transitional behavior from WD statistics toward Poisson statistics of eigenvalues has been captured by an exactly solvable model [108, 15]. This model incorporates a class of functions $V(\lambda)$ which transition from a strong to weak confining potential behavior, as a function of a *single* parameter. Consequently, this model defines a *one-parameter universality class* of RME's which generalizes that of classical (zero-parameter) RME's [95, 37]. The corresponding analytical work for orthogonal RME's with $\beta = 1$ (our focus here) is currently an open problem. However, numerical results [25] have shown that the statistical behavior of the RME's of both symmetry classes are qualitatively the same.

We point out that the random matrices we propose to study are of a different type than the classical RME. For our matrices $\chi_1 \Gamma \chi_1$, the randomness arises through the medium, as expressed through the matrix χ_1 , rather than by choosing the matrix entries directly according to some distribution.

3 Anderson Transition for Two Phase Composites

In RMT [72, 16, 37], long and short range correlations of the eigenvalues [25, 72] of random matrices are measured using various eigenvalue statistics [72, 16], such as the ESD, spectral rigidity, and number variance. The localization properties of the eigenvectors are measured in terms of quantities such as the inverse participation ratio (IPR) and the eigenvector entropy [115, 42]. In [102], we found that an Anderson-like transition to universality arises in the spectral characteristics of the random matrix $M = \chi_1 \Gamma \chi_1$ which governs the transport properties of two phase composites. We explored the transition in the 2D and 3D RRN, as well as in 2D discretizations of the brine microstructure of sea ice [64, 66, 63], melt ponds on Arctic sea ice [75], the sea ice pack itself (as shown in Fig. 2d–e), and porous human bone [68, 81, 17, 29].

To calculate the spectral measures for 2D images of sea ice and bone microstructure, we converted photographs to binary images corresponding to the two phases. For example, Fig. 2d–f displays binary images of the Arctic ice pack with varying degrees of ocean connectivity. The binary images were then mapped to high density resistor networks, from which the matrix $M = \chi_1 \Gamma \chi_1$ was then obtained.

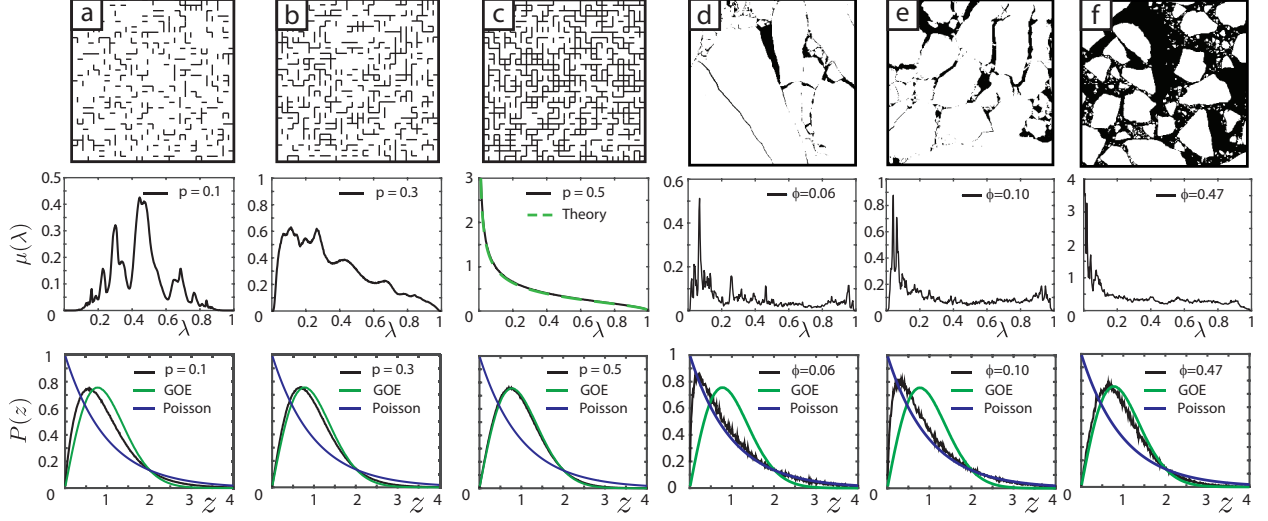


Figure 2: *Spectral upscaling for sea ice structures.* Increasingly connected configurations of the electrical percolation model (a)–(c), and leads in the ice pack (d)–(f), with corresponding spectral functions $\mu(\lambda)$ (histogram representations of the spectral measure) and eigenvalue spacing distributions (ESD) $P(z)$ below. The area under the graph of each spectral function in (d)–(f) is the open water fraction $\phi = 1 - \psi$. The eigenvalues in the ESD have been rescaled by an unfolding procedure to have unit mean spacing. For the network, the width of the gaps in the spectrum near $\lambda = 0, 1$ for $p = 0.1$ shrink to 0 as the percolation threshold $p = p_c = 0.5$ is approached, with a subsequent build up of spectra at $\lambda = 0$ as p surpasses p_c . The spectral functions for the ice pack exhibit a similar behavior.

The measure μ exhibits fascinating transitional behavior as a function of system connectivity. For example, in the case of a RRN with a low volume fraction p of open bonds, as shown in Fig. 2a, there are spectrum-free regions at the spectral endpoints $\lambda = 0, 1$ [106]. However, as p approaches the percolation threshold p_c [137, 148] and the system becomes increasingly connected, these spectral gaps shrink and then vanish [106, 80], as shown in Fig. 2a–c, leading to the formation of δ -components of μ at the spectral endpoints, *precisely* [106] when $p = p_c$ (and $p = 1 - p_c$ in $d = 3$). This leads to critical behavior of σ^* for insulating/conducting and conducting/superconducting systems [106]. This gap behavior of μ has led [60, 106] to a detailed description of these critical transitions in σ^* , which is directly analogous to the Lee–Yang–Ruelle–Baker description [7, 60] of the Ising model phase transition in the magnetization M . Moreover, using this gap behavior, all of the classical critical exponent scaling relations were recovered [106, 60] without heuristic scaling forms but instead by using the *rigorous* integral representation for σ^* involving μ .

Our computations of the ESD in Fig. 2 reveal a mechanism for the collapse in the spectral gaps of μ . For highly correlated WD spectra exhibited by, for example, real-symmetric matrices of the GOE, the nearest neighbor ESD $P(z)$ is accurately approximated by $P(z) \approx (\pi z/2) \exp(-\pi z^2/2)$, which illustrates *eigenvalue repulsion*, vanishing linearly as spacings $z \rightarrow 0$ [72, 139, 25]. In contrast, the ESD for uncorrelated Poisson spectra, $P(z) = \exp(-z)$, allows for level degeneracy [72]. In Fig. 2 we display the ESDs for Poisson and WD spectra, along with the ESDs for M corresponding to the 2D RRN with a fraction p of phase 1 and ice pack composites with fluid area fraction ϕ . It shows that for sparsely connected systems, the behavior of the ESDs is well described by weakly correlated Poisson-like statistics [25]. With increasing connectedness, the ESDs transition toward highly correlated WD statistics with strong level repulsion. For the 2D and 3D RRN, the eigenvalue density $\rho(\lambda, p)$ obeys $\rho(\lambda, p) = \rho(1 - \lambda, 1 - p)$ in the *bulk* of the spectrum. This is reflected in the ESDs by the symmetry $P(z, p) = P(z, 1 - p)$, as shown for the 2D RRN in Fig. 2a–c. Our computations of the spectral rigidity and number variance exhibit a similar transitional behavior [102].

Moreover, our computations of the ESD, spectral rigidity, and number variance for 3D RRN suggest that the GOE limit is attained by these eigenvalue statistics for *all* $p_c \leq p \leq 1 - p_c$, appearing to overlie the GOE limit almost exactly for all p values tested in $p_c \leq p \leq 1 - p_c$ as shown for ESDs in Fig. 3a. With this in mind, we recall the Anderson transition, where low disorder corresponds to extended states and WD statistics.

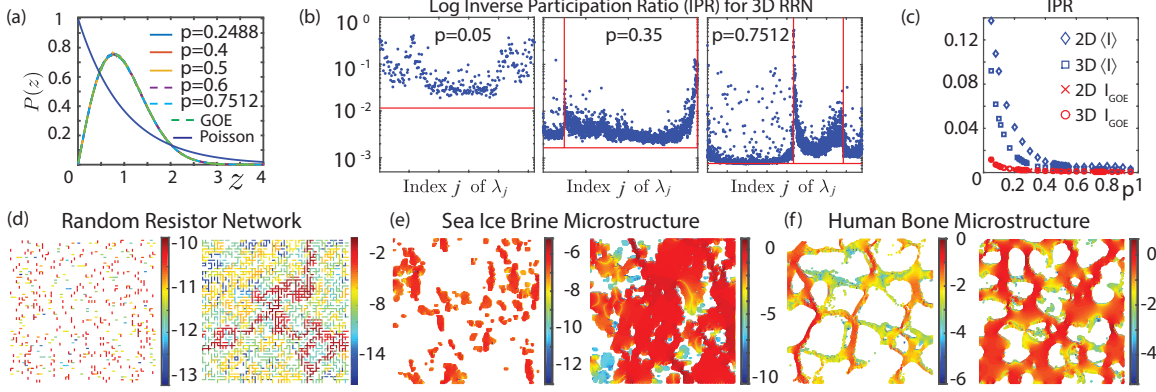


Figure 3: Spectral behavior of composite structures. (a) The ESDs for 3D RRN with $p_c \leq p \leq 1 - p_c$. (b) The IPR's of eigenvectors u_j associated with realizations of the 3D RRN plotted versus eigenvalue index j , with $L = 12$ and increasing values of p from left to right, with $1 - p_c \approx 0.7512$. The vertical lines define the δ -components of μ while the horizontal lines mark the IPR value $I_{GOE} = 3/N_1$ for the Gaussian orthogonal ensemble (GOE) with matrix size $N_1 \approx pN$, where $N = L^d d$. (c) The ensemble averaged IPR $\langle I \rangle$ as a function of p , displaying transitional behavior at the percolation thresholds, $p_c = 1/2$ for 2D and $p_c \approx 0.2488$ for 3D. (d)–(f) Electric fields (with logarithmic scale) in composite structures calculated via (4).

When disorder exceeds a critical level, the states localize and the eigenvalues become de-correlated. We view the 3D RRN with $p_c \leq p \leq 1 - p_c$ to be “ordered” with extended states and WD statistics. As p decreases, the disorder – or blockages to the flow – increases, and the eigenstates localize.

The eigenvectors u_j of $M = \chi_1 \Gamma \chi_1$, associated with the $N_1 \times N_1$ sub-matrices of Γ , also exhibit a connectedness driven transition in their localization properties. The IPR is defined as $I_j = \sum_i |u_j^i|^4$, $i, j = 1, \dots, N_1$, where u_j^i is the i th component of u_j . Eigenvectors of matrices in the GOE are known to be highly extended and independent of the eigenvalue distribution [37], and the IPR is given by $I_{GOE} = 3/N_1$ [115].

Equation (4) provides a direct link between localized eigenvectors u_j and eigenmodes of $\chi_1 E$ with large magnitudes in only a few resistors, while extended eigenvectors correspond to fields extending throughout the network. Fig. 3d-f shows our computations of the electric field $\chi_1 E$ for various composite structures.

Fig. 3b displays I_j for the 3D RRN plotted vs. index j , for various p values. In numerical simulations of finite RRN the δ -component at $\lambda = 0$ is manifested by a large number of λ_j with magnitude $\lesssim 10^{-14}$, followed by an abrupt change of magnitude $\gtrsim 10^{-4}$, with no eigenvalues in the interval $(10^{-14}, 10^{-4})$, and similarly for $\lambda = 1$. The locations of abrupt changes in eigenvalue magnitudes are identified by red vertical lines. The GOE IPR value is identified by the red horizontal line. This demonstrates that eigenvectors with the δ -components at $\lambda = 0, 1$ are more extended than others, with I_j values closer to the GOE limit.

This delocalization of the eigenvectors can be seen in Fig. 3c, which displays the p -dependence of $\langle I \rangle$ over all values of I_j . As p and system connectedness increase, $\langle I \rangle$ decreases, with transitional behavior at p_c , indicating that the eigenvectors (and eigenmodes of E), become extended throughout the network. Fig. 3b shows that this delocalization is largely due to the formation of δ -components in μ at $\lambda = 0, 1$.

Fig. 3b also shows that regions of extended states are separated by “mobility edges” with a sudden increase in the number of localized eigenvectors, which is analogous to Anderson localization, where mobility edges mark the characteristic energies of the MIT [72]. Remarkably, the mobility edges in Fig. 3b are precisely at the locations of the δ -components (red vertical lines) which control critical behavior in insulator/conductor and conductor/superconductor systems [106, 32, 13].

4 Proposed Research

Two phase composites and spectral measures. We have recently extended the mathematical framework discussed in Section 2 for two component media to compute the bulk transport coefficients associated with polycrystalline random media and advection enhanced diffusion. Stieltjes integral representations of the associated effective parameters involve a spectral measure of a self-adjoint random operator, which

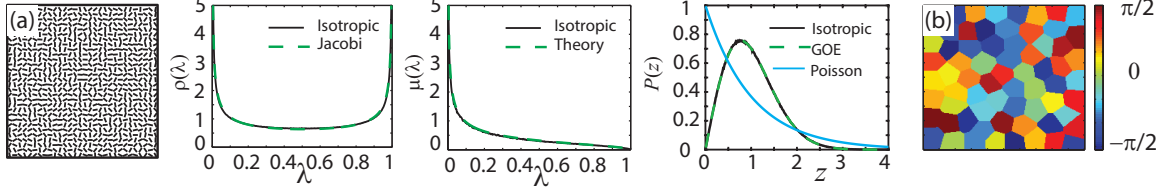


Figure 4: *Spectral analysis of polycrystalline media.* (a) A graphical, lattice representation of a polycrystalline medium which is isotropic within the horizontal plane, with the corresponding eigenvalue density $\rho(\lambda)$, spectral function $\mu(\lambda)$ (histogram representations of the spectral measure), and eigenvalue spacing distribution (ESD) to the right. The computed eigenvalue density $\rho(\lambda)$ is displayed with the limiting eigenvalue density for a Jacobi random matrix ensemble $\rho_J(\lambda) = 1/(\pi\sqrt{\lambda(1-\lambda)})$. The spectral function $\mu(\lambda)$ is displayed with its isotropic theoretical prediction [99] $\mu_I(\lambda) = (\sqrt{(1-\lambda)/\lambda})/\pi$. (b) Geometric shapes generated using a Voronoi diagram, with orientation angles uniformly distributed on the interval $(-\pi/2, \pi/2)$.

becomes a random matrix for discretizations of the continuum. A great deal of information can be gleaned about the effective transport properties of all three of these systems from the statistical behavior of the spectral measure, which itself is governed by the statistical properties of its associated eigenvalues λ_i and spectral weights m_i as well as the localization properties of eigenvectors u_i . We propose to analyze these systems and investigate their effective properties using methods of random matrix theory. We also propose to study the correlations of the λ_i and the m_i , the cross correlations between the λ_i and u_i , and other statistical measures to extract deeper insights into what controls effective transport in these systems.

As discussed in Section 2 the behavior of the spectral measure μ at the spectral end points is of central importance for two component media. We propose to investigate a possible analogue of the Tracy-Widom distribution of the largest and smallest eigenvalue associated with μ . Our recent numerical computations [105] of effective diffusivities for shear flow confirm the theoretical prediction [4] that the spectral measure is a delta function at the spectral origin. This is due to a concentration of masses m_i there, however the spectrum is spread out far away from the origin with near zero mass. The spectral behavior of eigenvalues for randomly perturbed shear flow is of key interest, which may lead to analytical solutions. Similarly, we plan to explore explicitly the spectral measure of the one dimensional RRN as system size increases.

Polycrystalline materials. Our recent analysis [73] of the electromagnetic transport properties of random, uniaxial polycrystalline media has demonstrated that the underlying, rigorous mathematical framework is a direct analogue of that for two-phase random media. For simplicity, we discuss the theory in terms of conductive polycrystalline materials, which are composed of many crystallites (single crystals of varying size, shape, and orientation) that can have different local conductivities along different crystal axes. In the case of uniaxial polycrystalline media, the local conductivity along one of the crystal axes has the *complex* value σ_1 , while the conductivity along all the other crystal axes have the value σ_2 . The local conductivity tensor of such media is given by [99, 9] $\sigma(x, \omega) = R^T \text{diag}(\sigma_1, \sigma_2, \dots, \sigma_2)R$, where $R(x, \omega)$ is a random rotation matrix, and σ can be written in a form which is a direct analogue of (3), involving the matrix $C = \text{diag}(1, 0, \dots, 0)$,

$$\sigma(x, \omega) = \sigma_1 X_1(x, \omega) + \sigma_2 X_2(x, \omega), \quad (9)$$

where $X_1 = R^T C R$ is a random projection matrix, $X_2 = I - X_1$, and $X_j X_k = X_i \delta_{jk}$, $j, k = 1, 2$.

The propagation properties of a quasistatic electromagnetic wave in a polycrystalline medium are determined by (1) (or analog $D = \epsilon E$ for permittivity), and the effective complex conductivity tensor σ^* is defined by (2). Moreover, in precise parallel with the two component setting, writing equation (9) as $\sigma = \sigma_2(I - X_1/s)$ yields the analogue of (4), $X_1 E = s(sI - X_1 \Gamma X_1)^{-1} X_1 e_k$, and a Stieltjes integral representation for the diagonal component $\sigma^* = \sigma_{kk}^*$ of σ^* , given by equation (5) with $F(s) = \langle [(sI - X_1 \Gamma X_1)^{-1} X_1 e_k] \cdot e_k \rangle$. Furthermore, the positive *spectral measure* μ on $[0, 1]$ is given by $\mu(d\lambda) = \langle Q(d\lambda) X_1 e_k \cdot e_k \rangle$ and $Q(d\lambda)$ is the (unique) projection valued measure associated with the random, bounded, self-adjoint operator $X_1 \Gamma X_1$ on $L^2(\Omega, P)$ with moments $\mu_n = \langle [(X_1 \Gamma X_1)^n e_k] \cdot e_k \rangle$. The mass $\mu_0 = \langle X_1 e_k \cdot e_k \rangle$ of μ can be thought of as the percentage of the crystals oriented in the k th direction e_k [73, 9]. We have developed a projection method analogous

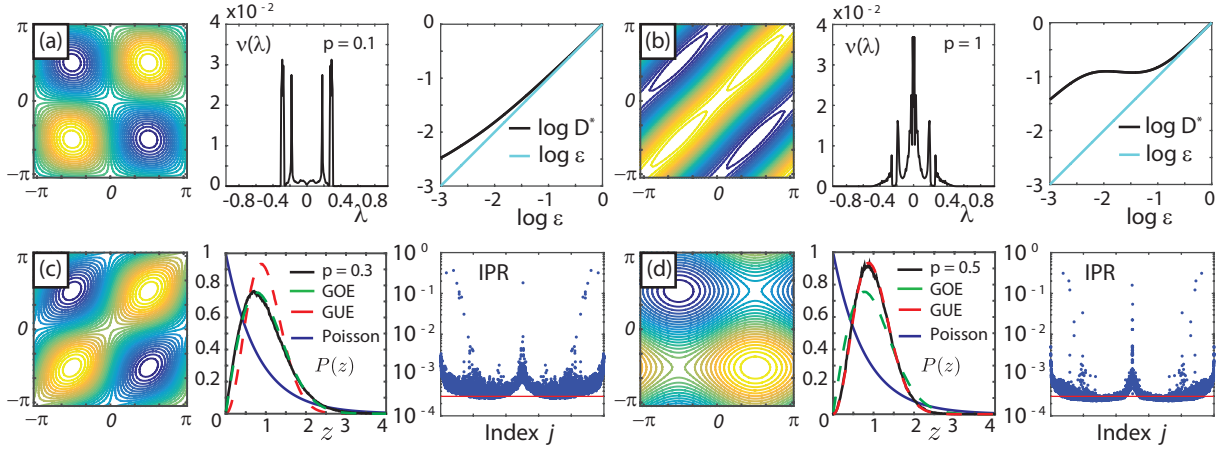


Figure 5: **Spectral behavior of effective diffusivities** (a)–(b) Random streamlines, spectral functions $\nu(\lambda)$ (histogram representations of the spectral measure), and the diagonal component $D^* = D_{11}^*$ of the effective diffusivity for cat's eye flow enhanced above the molecular diffusivity ε . The stream function is given by $H_{CE}(x, y) = \sin x \sin y + \xi \cos x \cos y$ with ξ uniformly distributed in the interval $(-p, p)$. (c)–(d) Streamlines, eigenvalue spacing distributions (ESD's), and inverse participation ratios (IPR's) for (c) cat's eye flow and (d) BC-flow with stream function $H_{BC}(x, y) = B \sin x - C \sin y$ with B and C uniformly distributed on $(-p, p)$.

to that in Section 2, enabling the direct computation of spectral measures, conductivities, fields, eigenvalue statistics, and eigenvector localization properties, as displayed in Fig. 4.

Via (7), we propose to directly compute spectral measures and effective conductivities corresponding to various polycrystal microstructures, such as random checkerboards and more realistic microstructures such as that displayed in Fig. 4(b), with various crystallite orientation statistics, and investigate the associated electromagnetic transport properties of sea ice as a polycrystalline medium. We will also explore the possible characterization of crystallite microstructures by geometric resonances in the measures, and transitions in the transport properties by behavior of spectral gaps, eigenvalue correlations, and eigenvector localization properties. An extension of the spectral coupling [27, 28, 29] in two component composites to polycrystalline media is also of key interest, so as to recover from the computed spectral measures, the electromagnetic and thermal transport properties of polycrystalline sea ice. A random matrix theory description of sea ice as a polycrystalline medium is a key part of our proposed work. A preliminary computation of the eigenvalue density $\rho(\lambda)$ corresponding to a two-dimensional polycrystalline medium with *statistically isotropic* crystallite orientation statistics is in striking agreement with the limiting eigenvalue density of a Jacobi random matrix ensemble, as shown in Fig. 4. This provides compelling evidence that the underlying random matrix is a member of this classical ensemble, which would open this problem up to a broad range of mathematical techniques [47, 37, 95]. We will investigate the possibility of an Anderson transition in the polycrystal spectral measure via a checkerboard model where the “crystals” are highly anisotropic, with the conducting direction in a square either vertical or horizontal with probability p or $1 - p$, and variations.

Advection diffusion. The analytic continuation method can be adapted to provide a Stieltjes integral for the effective diffusivity tensor D^* [3, 4, 105, 104], describing effective transport of a passive tracer T by a random, incompressible fluid velocity field v . The system is governed by the advection diffusion equation

$$\partial_t T = v \cdot \nabla T + \varepsilon \Delta T, \quad \nabla \cdot v = 0, \quad \langle v \rangle = 0. \quad (10)$$

Here $T(t, x, \omega)$ can be viewed as the local temperature, the positive constant ε represents the molecular diffusivity, $v(x, \omega)$ is a statistically homogeneous velocity field, and $\langle \cdot \rangle$ denotes statistical averaging. Since v is incompressible, it can be represented [3, 4] as $v = \nabla \cdot H$, where H is an antisymmetric matrix satisfying $H + H^T = 0$ and $\langle H \rangle = 0$. In terms of H , equation (10) takes the form of a diffusion equation $\partial_t T = \nabla \cdot [D \nabla T]$, where $D = \varepsilon I + H$ can be viewed as a local diffusivity matrix [3, 4].

In homogenization, we seek the long time, large distance behavior of solutions of (10). This introduces a small parameter δ , used to obtain a homogenized temperature [94], $\bar{T}(x, t) = \lim_{\delta \downarrow 0} T(x/\delta, t/\delta^2)$, satisfying a diffusion equation involving the *effective diffusivity tensor* D^* , $\partial_t \bar{T} = \nabla \cdot [D^* \nabla \bar{T}]$.

Remarkably, the effective diffusivity tensor D^* is obtained in terms of a *matrix* E which satisfies equation (1) with $J = DE$ and $\langle E \rangle = I$, and is given by $D^* \langle E \rangle = \varepsilon \langle E \cdot E \rangle$ [94, 4]. By the skew-symmetry of the matrix H , this formula is equivalent to equation (2) [43]. Again, due to the skew-symmetry of H the application of the spectral theorem must be slightly modified in this case [4]. The correspondence between the effective conductivity tensor σ^* and the effective diffusivity tensor D^* is given by

$$\sigma^* = \sigma_2 \left(I - \int_0^1 \frac{d\mu(\lambda)}{s - \lambda} \right), \quad D^* = \varepsilon \left(I + \int_{-\infty}^{\infty} \frac{d\nu(\tau)}{\varepsilon^2 + \tau^2} \right), \quad (11)$$

respectively, where μ and ν are matrix valued spectral measures associated with the self-adjoint operators $\chi_1 \Gamma \chi_1$ and $i \Gamma H \Gamma$. The first formula in (11) also holds for the uniaxial polycrystalline medium setting, where μ in this case is associated with the self-adjoint operator $X_1 \Gamma X_1$.

We have recently extended [105] our numerical methods discussed in Section 2 to compute the spectral measure ν for cat's eye flow, as well as the associated effective diffusivity D^* as a function ε , shown in Fig. 5(a) and (b). These computations show the spectral origin for advection-diffusion plays the role of the spectral endpoints for composite materials, with an increase in spectral mass giving rise to an advection-driven enhancement of effective diffusivity above the bare molecular diffusivity ε . This is a key example of how the behavior of the spectral measure ν governs the behavior of the bulk transport coefficient D^* . The behavior of ν is, in turn, governed by the statistical properties of the eigenvalues and eigenvectors of the matrix $i \Gamma H \Gamma$. A remarkable property of this matrix is that $\Gamma H \Gamma$ is *real-valued and anti-symmetric*, so the *Hermitian* matrix $i \Gamma H \Gamma$ is somewhat of a hybrid of real-symmetric and complex-symmetric matrices. This hybrid characteristic is illustrated by our spectral calculations of the ESD in Fig. 5 for (c) cat's eye flow [43] and (d) BC-flow [14], attaining that of the GOE and GUE, respectively. Our computations of the associated IPR in this figure exhibit regions of extended and localized states separated by *mobility edges*. We will use intuition gained from explorations of two phase media to explore how flow characteristics give rise to this spectral behavior and better understand how it enhances the effective diffusivity. Furthermore, we will more closely investigate the connections between flow geometry and spectral properties in order to construct examples which may exhibit an Anderson-like transition or other types of critical behavior.

RMT for multicomponent media. The integral representation for three phase media was first introduced in [59, 51], where bounds for the effective properties were obtained. For three-component media, functions of two complex variables $m(h_1, h_2)$ and $F(s_1, s_2) = 1 - m(h_1, h_2)$ with $h_i = \sigma_i / \sigma_3$, $s_i = 1 / (1 - h_i)$, $i = 1, 2$, were introduced. Cauchy's formula and special properties of holomorphic functions with their boundary values on a polydisc yield an integral representation with the measures supported on the torus T^2 .

Introducing $\zeta_j = \frac{s_j - i}{s_j + i}$, $j = 1, 2$, and $f(\zeta_1, \zeta_2) = iF(s_1, s_2)$ with $f(\zeta_1, \zeta_2) : D^2 \rightarrow \{Re f > 0\}$, where D^2 is a polydisc on \mathbb{C}^2 plane, $D^2 = \{|\zeta_1| < 1\} \times \{|\zeta_2| < 1\}$, in [51] it was shown that $f(\zeta_1, \zeta_2)$ is holomorphic with positive real part in D^2 , and it may be represented as

$$f(\zeta_1, \zeta_2) = iImf(0, 0) + \frac{1}{2} \int_0^{2\pi} \int_0^{2\pi} (H_1 H_2 + H_1 + H_2 - 1) \mu(dt_1, dt_2), \quad (12)$$

where the kernel is a combination of the functions $H_1 = (e^{it_1} + \zeta_1) / (e^{it_1} - \zeta_1)$ and $H_2 = (e^{it_2} + \zeta_2) / (e^{it_2} - \zeta_2)$, and μ is a positive Borel measure on the torus T^2 . Expansion of an operator representation for $F(s_1, s_2)$ [59, 51], into series allows characterization of extremal measures and construction of bounds for the effective properties of multiphase composites. A Fourier condition imposes constraints on admissible measures [51]. For example, while point measures on $[0, 1]$ are admissible and extremal for the two phase problem, a point mass on T^2 is not admissible. But the product of a point mass with Lebesgue measure is admissible and extremal on T^2 for the two phase problem, as are other **trajectories** on T^2 .

In the proposed work, we plan to investigate *trajectory statistics* for measures on T^2 for three phase composites as one phase percolates. The results will allow us to model different states of multiphase materials as well as to study behavior of the eigenstates in the phase transition. Based on this analysis, we will be able to link different phases and different scales in multiscale systems such as sea ice-slush-water system, important in ocean wave propagation, exhibiting composite structure on various scales.

We also propose to generalize the RMT mathematical framework to the polydisc integral representation on a torus for multi-axial polycrystalline media, with local, spatially varying conductivity tensor given by $\sigma = R^T \text{diag}(\sigma_1, \sigma_2, \sigma_3) R$, where R is a spatially varying rotation matrix. The polydisc representation in this

case will be derived similarly to the three-phase composite case. We conjecture that a highly anisotropic conductivity tensor with $\sigma_1 \gg \sigma_i, i = 2, 3$, may lead to an Anderson-like transition in the behavior of the fields in the composite when the strongly conducting component becomes connected. We hope to observe this phenomenon, similar to percolation, using numerical simulations. We will investigate statistics of the singularities of the measures on a torus in this transition and analyze the transitions in the eigenstates associated with grain growth in general polycrystalline materials.

Quasiperiodic media. In [56] it was discovered that homogenized classical transport coefficients of quasiperiodic media depend *discontinuously* on the wavelengths defining the medium. For example, consider a particle diffusing in a one dimensional potential $V(x) = \cos x + \cos kx, k \in \mathbb{R}$. Then the effective diffusion coefficient $D(k)$ has the same value D_0 for all irrational k , but differs from D_0 and depends on k for k rational. Thus $D(k)$ is discontinuous at rational k , and moreover, it is continuous at irrational k . This “pathology” is reflected in the length and time scales on which the system reaches its limiting behavior [56, 55]. These findings hold in general for all classical transport coefficients [56], and we constructed explicit examples of two phase composites in two dimensions that display this behavior [57, 53].

What is so interesting here is that what we originally found in [56] was viewed then as a type of classical analog of the rich spectral and localization behavior of Hamiltonians with quasiperiodic potentials [134, 135, 39]. The diffusion and conduction problems considered in [56], however, are governed by an elliptic PDE and not the Schrödinger wave equation. These results were somewhat surprising, in a way similar to finding an Anderson-like transition at a percolation threshold – in the absence of wave phenomena. We propose to investigate spectral statistics for the M matrix in the quasiperiodic case, motivated by [56].

Poissonian statistics in the dilute limit. For a purely homogeneous medium without random impurities the spectral measure is deterministic. In our setting it is a Dirac point mass supported entirely on 0 or 1 since $G = \Gamma$ is a projection operator. With the introduction of a small amount of randomness the spectral measure becomes random and supported on $[0, 1]$, yet should still only be a small random perturbation away from the deterministic measure of the homogeneous model.

A major goal is to determine the statistics of this random perturbation, in the rescaled limit as the randomness vanishes, the so-called *dilute limit*. We have strong reason to believe that the dilute limit exhibits *Poissonian statistics*. Eigenvalues obeying Poissonian statistics are independent of each other and exhibit very weak repulsion, resulting in their spacing distribution following an exponential density. For random Schrödinger operators and related models it is well known [101, 84, 85] that Poissonian statistics appear in the dilute limit, with the analysis using tools from transfer matrices, orthogonal polynomials, and matrix ensembles built up from independent inputs. For the spectral measures here the corresponding matrix ensembles are of a different nature and require a new type of analysis.

Fig. 2 exhibits the eigenvalue statistics for a discrete composite determined by the percolation model on \mathbb{Z}^2 . The spectral measure $\mu(\lambda)$ is for the random self-adjoint operator $\chi_1 \Gamma \chi_1$, where Γ is the projection operator taking functions on edges into the space of curl free functions on the edges (the so-called bond space). The operator χ_1 zeros out rows and columns of Γ corresponding to the deleted edges of the percolation configuration and is the only source of randomness in the operator. When $p \rightarrow 0$ the eigenvalues cluster near zero and it is expected that they become independent of each other and governed by Poisson statistics. Our project will attempt to prove this by computing the Jacobi tridiagonal matrix of the operator $\chi_1 \Gamma \chi_1$ via the Householder transformation. The law of the random Jacobi coefficients a_n, b_n fully determines the law of the random spectral measure via the associated orthogonal polynomials, and while these laws are likely not explicit in our case we are confident that the asymptotics can be analyzed as $p \rightarrow 0$. This is similar to the approach in [100, 101, 88, 76] for random Schrödinger operators and the Anderson model, which we are confident can be adapted to our situation.

Conformal invariance and universality. For the \mathbb{Z}^2 percolation model the last 15 years have seen remarkable progress in the development and understanding of scaling limits for percolation clusters using the Schramm-Loewner evolution [126, 121, 151, 136, 24] and Conformal Loop Ensembles [131, 132, 23, 82]. Although the scaling limit result has only been proven for site percolation on the hexagonal lattice it is believed to hold in fuller generality, and in particular should also be present in our model. A crucial property of these scaling limits is their *conformal invariance* properties, namely that the law of the clusters restricted to one domain is the conformal image of the law of clusters from another domain via the Riemann mapping that connects the domains. This suggests that some sort of conformal invariance should also be present in

the spectral measure, and one of the main goals of the project will be to find it. Another interesting aspect is if within the spectral measure one can observe the universal critical exponents β and ν for the density of the infinite cluster and the correlation length, respectively. At this point this is purely speculative but not unreasonable. From a composite materials point of view the spectral measure encodes all properties of the material, which in this case come from the geometry of the percolation clusters. Inverting the spectral measure to analyze these exponents may be possible and we will investigate in this direction.

An interesting question raised by our approach is if the spectral measures of the discretized systems we study actually depend on the choice of discretization, specifically on the choice of lattice. For percolation models it is widely believed that the critical exponent t for conductivity, the correlation length exponent ν and the cluster density exponent β are universal in the sense that they are the same on every reasonable lattice. Given this, one should also expect that the spectral measure we propose to study exhibits universal behavior with respect to the choice of lattice. Our investigations thus far have been for the square lattice, but as part of the proposed project we will study the spectral measure on related regular lattices such as hexagonal and isoradial lattices in two dimensions and the permutahedron in three dimensions. Another interesting direction is whether we can “see” the critical percolation exponents within the spectral measure itself, which would be a completely new way of studying them.

What do our findings say about real composites? To help connect our findings in [102] to the physics of disordered media, we consider two systems whose optical properties are determined by the spectral characteristics considered here, and where our findings may have observable consequences: metallic particles in an insulating host, such as colloidal suspensions of gold nanoparticles in a liquid [13], and metal films such as depositions of nanosized metal particles on a dielectric substrate [49]. The long wavelength quasistatic assumption holds in the visible range, and these systems are described macroscopically by an effective complex permittivity ϵ^* , and locally by the elliptic PDE with local complex permittivity values $\epsilon_1(\omega)$ and $\epsilon_2(\omega)$ (here ω is angular frequency). Values of $h = \epsilon_1/\epsilon_2$ near the negative real axis can be realized in these systems over certain ranges of frequency ω [13]. In general, the locations of the eigenvalues along the negative real axis correspond to singularities of the transport coefficients [99, 13, 80, 32]. The resonance structure of ϵ^* and the absorption profile, such as sharp peaks associated with *surface plasmon resonances* [13, 49], are observable [13, 32] and determined by the spectral properties of G . For finite discrete models such as $RL - C$ networks [13, 49, 32, 80], the eigenvalues of the matrix M are poles of the effective complex conductivity which collectively give rise to network resonances. Our findings on the transition to *universality* of the resonance spacing distribution, for example, may be observable through analysis of the fine structure of the absorption spectra. Interestingly, WD universality has been observed in microwave absorption spectra of a suspension of metal particles at low temperature, where the energy level spacing distribution for electronic states in the grains determines the conductivity [157]. We plan to analyze models of metal-insulator composites for physical consequences of the Anderson-like transition.

We propose to explore the large scale effective transport properties of the ice pack and configurations of ice floes, through the lens of random matrix theory and the evolution of eigenvalue statistics and spectral measures. This approach will yield fundamental new insights into the relationship between geometric resonances in the measures and floe geometry, as well as transitions in eigenvalue correlations and spectral gaps in the measures and the percolation properties of floe configurations. This work will help provide a rigorous way of upscaling microstructural information to larger scales which are relevant to climate models.

5 Broader impacts

Portions of the funds will be used to partially support a graduate student and undergraduates, thus introducing them to this highly interdisciplinary research area. PI Golden has developed a new upper division course, Math 5750 / 6880 on Mathematics and Climate, and will incorporate some of this research on random matrix theory for sea ice structures into this course. Finally, it is likely that there will be some media interest in this work, extending the impact beyond traditional academic channels, particularly on the implications for sea ice structures in the climate system (there has already been media interest in our early results on universal behavior of spectral properties in the sea ice context).

References

- [1] M. Adler and P. Van Moerbeke. PDEs for the joint distributions of the Dyson, Airy and Sine processes. *The Annals of Probability*, 33(4):1326–1361, 2005.
- [2] P. Anderson. Absence of diffusion in certain random lattices. *Phys. Rev.*, 109:1492–1505, 1958.
- [3] M. Avellaneda and A. Majda. Stieltjes integral representation and effective diffusivity bounds for turbulent transport. *Phys. Rev. Lett.*, 62:753–755, 1989.
- [4] M. Avellaneda and A. Majda. An integral representation and bounds on the effective diffusivity in passive advection by laminar and turbulent flow. *Comm. Math. Phys.*, 138:339–391, 1991.
- [5] M. Avellaneda and M. Vergassola. Stieltjes integral representation of effective diffusivities in time-dependent flows. *Phys. Rev. E*, 52(3):3249–3251, 1995.
- [6] Z. Bai and Y. Yin. Convergence to the semicircle law. *The Annals of Probability*, pages 863–875, 1988.
- [7] G. A. Baker. *Quantitative Theory of Critical Phenomena*. Academic Press, New York, 1990.
- [8] J. N. Bandyopadhyay and S. Jalan. Universality in complex networks: random matrix analysis. *Phys. Rev. E*, 76:026109 (4pp.), 2007.
- [9] S. Barabash and D. Stroud. Spectral representation for the effective macroscopic response of a polycrystal: application to third-order non-linear susceptibility. *J. Phys., Condens. Matter*, 11:10323–10334, 1999.
- [10] M. Barjatia, T. Tasdizen, B. Song, C. Sampson, and K. M. Golden. Network modeling of arctic melt ponds. *Cold Regions Science and Technology*, 124:40–53, 2016.
- [11] D. J. Bergman. The dielectric constant of a composite material – A problem in classical physics. *Phys. Rep. C*, 43(9):377–407, 1978.
- [12] D. J. Bergman. Exactly solvable microscopic geometries and rigorous bounds for the complex dielectric constant of a two-component composite material. *Phys. Rev. Lett.*, 44:1285–1287, 1980.
- [13] D. J. Bergman and D. Stroud. Physical properties of macroscopically inhomogeneous media. *Solid State Phys.*, 46:147–269, 1992.
- [14] L. Biferale, A. Crisanti, M. Vergassola, and A. Vulpiani. Eddy diffusivities in scalar transport. *Phys. Fluids*, 7:2725–2734, 1995.
- [15] C. Blecken, Y. Chen, and K. A. Muttalib. Transitions in spectral statistics. *J. Phys. A: Math. Gen.*, 27(16):L563, 1994.
- [16] O. Bohigas and M.-J. Giannoni. Chaotic motion and random matrix theories. In *Mathematical and Computational Methods in Nuclear Physics (Granada, 1983)*, volume 209 of *Lecture Notes in Phys.*, pages 1–99. Springer, Berlin, 1984.
- [17] C. Bonifasi-Lista and E. Cherkaev. Electrical impedance spectroscopy as a potential tool for recovering bone porosity. *Phys. Med. Biol.*, 54(10):3063–3082, 2009.
- [18] J.-P. Bouchaud and M. Potters. Financial applications of random matrix theory: a short review. *arXiv preprint arXiv:0910.1205*, 2009.
- [19] B. Bowen, C. Strong, and K. M. Golden. Modeling the fractal geometry of Arctic melt ponds using the level sets of random surfaces. Invited submission for *Journal of Fractal Geometry*, 21 pp., under review, 2016.

- [20] S. R. Broadbent and J. M. Hammersley. Percolation processes I. Crystals and mazes. *Proc. Cambridge Philos. Soc.*, 53:629–641, 1957.
- [21] O. Bruno and K. Golden. Interchangeability and bounds on the effective conductivity of the square lattice. *J. Stat. Phys.*, 61:365, 1990.
- [22] A. Bunde and S. Havlin, editors. *Fractals and Disordered Systems*. Springer-Verlag, New York, 1991.
- [23] F. Camia and C.M. Newman. Two-dimensional critical percolation: the full scaling limit. *Comm. Math. Phys.*, 268(1):1–38, 2006.
- [24] F. Camia and C.M. Newman. Critical percolation exploration path and SLE_6 : a proof of convergence. *Probab. Theory Related Fields*, 139(3-4):473–519, 2007.
- [25] C. M. Canali. Model for a random-matrix description of the energy-level statistics of disordered systems at the Anderson transition. *Phys. Rev. B*, 53(7):3713–3730, 1996.
- [26] J. T. Chayes and L. Chayes. Bulk transport properties and exponent inequalities for random resistor and flow networks. *Comm. Math. Phys.*, 105:133–152, 1986.
- [27] E. Cherkaev. Inverse homogenization for evaluation of effective properties of a mixture. *Inverse Problems*, 17:1203–1218, 2001.
- [28] E. Cherkaev. Spectral coupling of effective properties of a random mixture. In A. B. Movchan, editor, *IUTAM Symposium on Asymptotics, Singularities and Homogenisation in Problems of Mechanics*, volume 113 of *Solid Mechanics and Its Applications*, pages 331–340. Springer Netherlands, 2004.
- [29] E. Cherkaev and C. Bonifasi-Lista. Characterization of structure and properties of bone by spectral measure method. *J. Biomech.*, 44(2):345–351, 2011.
- [30] K. Christensen and N. R. Moloney. *Complexity and Criticality*. Imperial College Press, London, 2005.
- [31] F.R.K. Chung, L. Lu, Conference Board of the Mathematical Sciences, and National Science Foundation (U.S.). *Complex Graphs and Networks*. Number no. 107 in *Complex graphs and networks*. American Mathematical Society, 2006.
- [32] J. P. Clerc, G. Giraud, J. M. Laugier, and J. M. Luck. The electrical conductivity of binary disordered systems, percolation clusters, fractals and related models. *Adv. Phys.*, 39(3):191–309, 1990.
- [33] A. Coniglio. Fractal structure of Ising and Potts clusters: Exact results. *Phys. Rev. Lett.*, 62(26):3054–3057, 1989.
- [34] J.L. Tison S. F. Ackley D. Liu, J. Zhu and K. M. Golden. Inversion schemes for recovering the thermal conductivity of sea ice from temperature data. 20 pp., Submitted, 2016.
- [35] A. R. Day and M. F. Thorpe. The spectral function of random resistor networks. *J. Phys.: Cond. Matt.*, 8:4389–4409, 1996.
- [36] P. Deift. *Orthogonal Polynomials and Random Matrices: a Riemann–Hilbert Approach*. Courant Institute of Mathematical Sciences, New York, NY, 2000.
- [37] P. Deift. *Random Matrix Theory: Invariant Ensembles and Universality*. Courant Institute of Mathematical Sciences, New York, NY, 2009.
- [38] D. Delande. Les Houches, école d’été de physique théorique. In M. J. Giannoni, A. Voros, and J. Zinn-Justin, editors, *Chaos et Physique Quantique—Chaos and Quantum Physics = Les Houches, session LII, 1–31 août 1989*, pages 665–726. North-Holland, Amsterdam, 1991.
- [39] F. Delyon, Y. Levy, and B. Souillard. Anderson localization for multi-dimensional systems at large disorder or large energy. *Comm. Math. Phys.*, 100:463–470, 1985.

- [40] F.J. Dyson. A Brownian-motion model for the eigenvalues of a random matrix. *Journal of Mathematical Physics*, 3(6):1191–1198, 1962.
- [41] H. Eicken, T. C. Grenfell, D. K. Perovich, J. A. Richter-Menge, and K. Frey. Hydraulic controls of summer Arctic pack ice albedo. *J. Geophys. Res. (Oceans)*, 109(C18):C08007.1–C08007.12, 2004.
- [42] F. Evers and A. D. Mirlin. Anderson transitions. *Rev. Mod. Phys.*, 80(4):1355–1418, 2008.
- [43] A. Fannjiang and G. Papanicolaou. Convection enhanced diffusion for periodic flows. *SIAM Journal on Applied Mathematics*, 54(2):333–408, 1994.
- [44] A. Fannjiang and G. Papanicolaou. Convection-enhanced diffusion for random flows. *J. Stat. Phys.*, 88(5-6):1033–1076, 1997.
- [45] S. Feng, B. I. Halperin, and P. N. Sen. Transport properties of continuum systems near the percolation threshold. *Phys. Rev. B*, 35:197–214, 1987.
- [46] D. Flocco, D. L. Feltham, and A. K. Turner. Incorporation of a physically based melt pond scheme into the sea ice component of a climate model. *J. Geophys. Res.*, 115:C08012 (14 pp.), doi:10.1029/2009JC005568, 2010.
- [47] P. J. Forrester. *Log-gases and random matrices*. Princeton University Press, Princeton, New Jersey, 2010.
- [48] K. E. Frey, D. K. Perovich, and B. Light. The spatial distribution of solar radiation under a melting Arctic sea ice cover. *Geophys. Res. Lett.*, 38:L22501, doi:10.1029/2011GL049421, 2011.
- [49] D. A. Genov, V. M. Shalaev, and A. K. Sarychev. Surface plasmon excitation and correlation-induced localization-delocalization transition in semicontinuous metal films. *Phys. Rev. B*, 72:113102–1–113102–4, 2005.
- [50] A. Goia and P. Vieu. An introduction to recent advances in high/infinite dimensional statistics [Editorial]. *J. Multivariate Anal.*, 146:1–6, 2016.
- [51] K. Golden. Bounds on the complex permittivity of a multicomponent material. *J. Mech. Phys. Solids*, 34(4):333–358, 1986.
- [52] K. Golden. Convexity and exponent inequalities for conduction near percolation. *Phys. Rev. Lett.*, 65(24):2923–2926, 1990.
- [53] K. Golden. Classical transport in quasiperiodic media. In W. Kohler and B. White, editors, *Proceedings of AMS-SIAM Summer Seminar on the Mathematics of Random Media*. AMS-SIAM, 1991.
- [54] K. Golden. Exponent inequalities for the bulk conductivity of a hierarchical model. *Comm. Math. Phys.*, 43(3):467–499, 1992.
- [55] K. Golden and S. Goldstein. Arbitrarily slow decay of correlations in quasiperiodic systems. *J. Stat. Phys.*, 52:1113–1118, 1988.
- [56] K. Golden, S. Goldstein, and J. L. Lebowitz. Classical transport in modulated structures. *Phys. Rev. Lett.*, 55:2629–2632, 1985.
- [57] K. Golden, S. Goldstein, and J. L. Lebowitz. Discontinuous behavior of effective transport coefficients in quasiperiodic media. *J. Stat. Phys.*, 58:669–684, 1990.
- [58] K. Golden and G. Papanicolaou. Bounds for effective parameters of heterogeneous media by analytic continuation. *Comm. Math. Phys.*, 90:473–491, 1983.
- [59] K. Golden and G. Papanicolaou. Bounds for effective parameters of multicomponent media by analytic continuation. *J. Stat. Phys.*, 40(5/6):655–667, 1985.

- [60] K. M. Golden. Critical behavior of transport in lattice and continuum percolation models. *Phys. Rev. Lett.*, 78(20):3935–3938, 1997.
- [61] K. M. Golden. The interaction of microwaves with sea ice. In G. Papanicolaou, editor, *Wave Propagation in Complex Media, IMA Volumes in Mathematics and its Applications, Vol. 96*, pages 75 – 94. Springer – Verlag, 1997.
- [62] K. M. Golden. Percolation models for porous media. In U. Hornung, editor, *Homogenization and Porous Media*, pages 27 – 43. Springer – Verlag, 1997.
- [63] K. M. Golden. Climate change and the mathematics of transport in sea ice. *Notices of the American Mathematical Society*, 56(5):562–584 and issue cover, 2009.
- [64] K. M. Golden, S. F. Ackley, and V. I. Lytle. The percolation phase transition in sea ice. *Science*, 282:2238–2241, 1998.
- [65] K. M. Golden, H. Eicken, A. Gully, M. Ingham, K. A. Jones, J. Lin, J. Reid, C. Sampson, and A. P. Worby. Electrical signature of the percolation threshold in sea ice. Submitted, 2016.
- [66] K. M. Golden, H. Eicken, A. L. Heaton, J. Miner, D. Pringle, and J. Zhu. Thermal evolution of permeability and microstructure in sea ice. *Geophys. Res. Lett.*, 34:L16501 (6 pages and issue cover), doi:10.1029/2007GL030447, 2007.
- [67] K. M. Golden, A. Gully, C. S. Sampson, D. J. Lubbers, and J.L. Tison. Percolation threshold for fluid permeability in antarctic granular sea ice. Preprint, 12 pp., 2016.
- [68] K. M. Golden, N. B. Murphy, and E. Cherkaev. Spectral analysis and connectivity of porous microstructures in bone. *J. Biomech.*, 44:337–344, 2011.
- [69] G. Grimmett. *Percolation*. Springer-Verlag, New York, 1989.
- [70] Y. Gu, K. W. Yu, and Z. R. Yang. Fluctuations and scaling of inverse participation ratios in random binary resonant composites. *Phys. Rev. B*, 66(1):012202, 2002.
- [71] Y. Gu, K. W. Yu, and Z. R. Yang. Statistics of level spacing of geometric resonances in random binary composites. *Phys. Rev. E*, 65:046129 (5pp.), 2002.
- [72] T. Guhr, A. Müller-Groeling, and H. A. Weidenmüller. Random-matrix theories in quantum physics: Common concepts. *Phys. Rept.*, 299(4–6):189–425, June 1998.
- [73] A. Gully, J. Lin, E. Cherkaev, and K. M. Golden. Bounds on the complex permittivity of polycrystalline composites by analytic continuation. *Proc. Roy. Soc. London A*, 471(2174):17 pp., doi: 10.1098/rspa.2014.0702 (including cover), 2015.
- [74] B. I. Halperin, S. Feng, and P. N. Sen. Differences between lattice and continuum percolation transport exponents. *Phys. Rev. Lett.*, 54(22):2391–2394, 1985.
- [75] C. Hohenegger, B. Alali, K. R. Steffen, D. K. Perovich, and K. M. Golden. Transition in the fractal geometry of Arctic melt ponds. *The Cryosphere*, 6(5):1157–1162, 2012.
- [76] François J.-M. Combes, F. Germinet and A. Klein. Poisson statistics for eigenvalues of continuum random Schrödinger operators. *Anal. PDE*, 3(1):49–80, 2010.
- [77] J. D. Jackson. *Classical Electrodynamics*. John Wiley and Sons, Inc., New York, 1999.
- [78] S. Jalan and J. N. Bandyopadhyay. Random matrix analysis of network laplacians. *Phys. A*, 387(2–3):667 – 674, 2008.
- [79] I.M. Johnstone. High dimensional statistical inference and random matrices. In *International Congress of Mathematicians. Vol. I*, pages 307–333. Eur. Math. Soc., Zürich, 2007.

- [80] T. Jonckheere and J. M. Luck. Dielectric resonances of binary random networks. *J. Phys. A: Math. Gen.*, 31:3687–3717, 1998.
- [81] J. Kabel, A. Odgaard, B. van Rietbergen, and R. Huiskes. Connectivity and the elastic properties of cancellous bone. *Bone*, 24(2):115–120, 1999.
- [82] A. Kemppainen and W. Werner. The nested simple conformal loop ensembles in the Riemann sphere. *Probab. Theory Related Fields*, 165(3-4):835–866, 2016.
- [83] A. R. Kerstein. Equivalence of the void percolation problem for overlapping spheres and a network problem. *J. Phys. A*, 16:3071–3075, 1983.
- [84] R. Killip and F. Nakano. Eigenfunction statistics in the localized Anderson model. *Ann. Henri Poincaré*, 8(1):27–36, 2007.
- [85] R. Killip and M. Stoiciu. Eigenvalue statistics for CMV matrices: from Poisson to clock via random matrix ensembles. *Duke Math. J.*, 146(3):361–399, 2009.
- [86] V. E. Kravtsov and K. A. Muttalib. New class of random matrix ensembles with multifractal eigenvectors. *Phys. Rev. Lett.*, 79(10):1913–1916, 1997.
- [87] T. Kriecherbauer, J. Marklof, and A. Soshnikov. Random matrices and quantum chaos. *Proceedings of the National Academy of Sciences*, 98(19):10531–10532, 2001.
- [88] E. Kritchevski. Poisson statistics of eigenvalues in the hierarchical Anderson model. *Ann. Henri Poincaré*, 9(4):685–709, 2008.
- [89] M. Potters Marc L. Laloux, P. Cizeau and J.-P. Bouchaud. Random matrix theory and financial correlations. *International Journal of Theoretical and Applied Finance*, 3(03):391–397, 2000.
- [90] F. Luo, Y. Yang, J. Zhong, H. Gao, L. Khan, D. Thompson, and J. Zhou. Constructing gene co-expression networks and predicting functions of unknown genes by random matrix theory. *BMC Bioinformatics*, 8(1), 2007.
- [91] Y. Ma, I. Sudakov, C. Strong, and K. M. Golden. Ising model for melt ponds on arctic sea ice. Preprint, 2016.
- [92] A. Majda and P. R. Kramer. *Simplified Models for Turbulent Diffusion: Theory, Numerical Modelling, and Physical Phenomena*. Physics reports. North-Holland, 1999.
- [93] A. J. Majda and P. E. Souganidis. Large scale front dynamics for turbulent reaction-diffusion equations with separated velocity scales. *Nonlinearity*, 7(1):1–30, 1994.
- [94] D. McLaughlin, G. Papanicolaou, and O. Pironneau. Convection of microstructure and related problems. *SIAM J. Appl. Math.*, 45:780–797, 1985.
- [95] M. L. Mehta. *Random Matrices*. Elsevier, Amsterdam, third edition, 2004.
- [96] J. A. Méndez-Bermúdez, A. Alcazar-López, A. J. Martínez-Mendoza, Francisco A. Rodrigues, and Thomas K. DM. Peron. Universality in the spectral and eigenfunction properties of random networks. *Phys. Rev. E*, 91(3):032122, Mar 2015.
- [97] F. Mezzadri and N. C. Snaith. *Recent Perspectives in Random Matrix Theory and Number Theory*. Cambridge University Press, Cambridge, UK, 2005.
- [98] G. W. Milton. Bounds on the complex dielectric constant of a composite material. *Appl. Phys. Lett.*, 37:300–302, 1980.
- [99] G. W. Milton. *Theory of Composites*. Cambridge University Press, Cambridge, 2002.
- [100] N. Minami. Local fluctuation of the spectrum of a multidimensional Anderson tight binding model. *Comm. Math. Phys.*, 177(3):709–725, 1996.

- [101] S. A. Molčanov. The local structure of the spectrum of the one-dimensional Schrödinger operator. *Comm. Math. Phys.*, 78(3):429–446, 1980/81.
- [102] N. B. Murphy, E. Cherkaev, and K. M. Golden. Anderson transition for classical transport in composite materials. 6 pp., Submitted, 2016.
- [103] N. B. Murphy, E. Cherkaev, C. Hohenegger, and K. M. Golden. Spectral measure computations for composite materials. *Commun. Math. Sci.*, 13(4):825–862, 2015.
- [104] N. B. Murphy, E. Cherkaev, J. Xin, J. Zhu, and K. M. Golden. Spectral analysis and computation of effective diffusivities in space-time periodic incompressible flows. *Annals of Mathematical Sciences and Applications*, 64 pp., in press, 2016.
- [105] N. B. Murphy, E. Cherkaev, J. Zhu, J. Xin, and K. M. Golden. Spectral analysis and computation of effective diffusivities for steady random flows. 42 pp., Submitted, 2016.
- [106] N. B. Murphy and K. M. Golden. The Ising model and critical behavior of transport in binary composite media. *J. Math. Phys.*, 53:063506 (25pp.), 2012.
- [107] N. B. Murphy, C. Hohenegger, C. S. Sampson, B. Alali, K. Steffen, D. K. Perovich, H. Eicken, and K. M. Golden. Spectral analysis of multiscale sea ice structures in the climate system. In preparation, 2016.
- [108] K. A. Muttalib, Y. Chen, M. E. H. Ismail, and V. N. Nicopoulos. New family of unitary random matrices. *Phys. Rev. Lett.*, 71(4):471–475, 1993.
- [109] C. Orum, E. Cherkaev, and K. M. Golden. Recovery of inclusion separations in strongly heterogeneous composites from effective property measurements. *Proc. Roy. Soc. London A*, 468(2139):784–809, 2012.
- [110] G. Palla and G. Vattay. Spectral transitions in networks. *New J. Phys.*, 8(307), 2006.
- [111] D. Paul and A. Aue. Random matrix theory in statistics: a review. *J. Statist. Plann. Inference*, 150:1–29, 2014.
- [112] G. A. Pavliotis. *Homogenization theory for advection-diffusion equations with mean flow*. PhD thesis, Rensselaer Polytechnic Institute Troy, New York, 2002.
- [113] C. A. Pedersen, E. Roeckner, M. Lüthje, and J. Winther. A new sea ice albedo scheme including melt ponds for ECHAM5 general circulation model. *J. Geophys. Res.*, 114:D08101, doi:10.1029/2008JD010440, 2009.
- [114] D. K. Perovich, J. A. Richter-Menge, K. F. Jones, and B. Light. Sunlight, water, and ice: Extreme Arctic sea ice melt during the summer of 2007. *Geophys. Res. Lett.*, 35:L11501, doi:10.1029/2008GL034007, 2008.
- [115] V. Plerou, P. Gopikrishnan, B. Rosenow, L. A. N. Amaral, T. Guhr, and H. E. Stanley. Random matrix approach to cross correlations in financial data. *Phys. Rev. E*, 65(6):066126, Jun 2002.
- [116] C. Polashenski, K. M. Golden, D. K. Perovich, E. Skillingstad, A. Arnsten, C. Stwertka, and N. Wright. Percolation blockage: A process that enables melt pond formation on first year Arctic sea ice. *Journal of Geophysical Research (Oceans)*, 74 pp., under review, 2016.
- [117] C. Polashenski, D. Perovich, and Z. Courville. The mechanisms of sea ice melt pond formation and evolution. *J. Geophys. Res. C (Oceans)*, 117:C01001 (23 pp.), doi:10.1029/2011JC007231, 2012.
- [118] D. J. Pringle, J. E. Miner, H. Eicken, and K. M. Golden. Pore-space percolation in sea ice single crystals. *J. Geophys. Res. (Oceans)*, 114:C12017, 12 pp., doi:10.1029/2008JC005145, 2009.
- [119] K. Rajan and L.F. Abbott. Eigenvalue spectra of random matrices for neural networks. *Phys. Rev. Lett.*, 97:188104, Nov 2006.

- [120] M. C. Reed and B. Simon. *Functional Analysis*. Academic Press, San Diego CA, 1980.
- [121] S. Rohde and O. Schramm. Basic properties of SLE. *Ann. of Math. (2)*, 161(2):883–924, 2005.
- [122] H Sagan. *Space-Filling Curves*. Springer Verlag, New York, 1994.
- [123] M. Sahimi. *Applications of Percolation Theory*. Taylor and Francis Ltd., London, 1994.
- [124] M. Sahimi. *Flow and Transport in Porous Media and Fractured Rock*. VCH, Weinheim, 1995.
- [125] J. Sakhr and J. M. Nieminen. Poisson-to-Wigner crossover transition in the nearest-neighbor statistics of random points on fractals. *Phys. Rev. E*, 72(4):045204, Oct 2005.
- [126] O. Schramm. Scaling limits of loop-erased random walks and uniform spanning trees. *Israel J. Math.*, 118:221–288, 2000.
- [127] F. Scott and D. L. Feltham. A model of the three-dimensional evolution of Arctic melt ponds on first-year and multiyear sea ice. *J. Geophys. Res.*, 115:C12064, doi:10.1029/2010JC006156, 2010.
- [128] M. Segev, Y. Silberberg, and D. N. Christodoulides. Anderson localization of light. *Nature Photonics*, 7:197–204, 2013.
- [129] T. H. Seligman, J. J. M. Verbaarschot, and M. R. Zirnbauer. Quantum spectra and transition from regular to chaotic classical motion. *Phys. Rev. Lett.*, 53(3):215–217, Jul 1984.
- [130] T. H. Seligman, J. J. M. Verbaarschot, and M. R. Zirnbauer. Spectral fluctuation properties of Hamiltonian systems: the transition region between order and chaos. *J. Phys. A: Math. Gen.*, 18:2751–2770, 1985.
- [131] S. Sheffield. Exploration trees and conformal loop ensembles. *Duke Math. J.*, 147(1):79–129, 2009.
- [132] S. Sheffield and W. Werner. Conformal loop ensembles: the Markovian characterization and the loop-soup construction. *Ann. of Math. (2)*, 176(3):1827–1917, 2012.
- [133] B. I. Shklovskii, B. Shapiro, B. R. Sears, P. Lambrianides, and H. B. Shore. Statistics of spectra of disordered systems near the metal-insulator transition. *Phys. Rev. B*, 47(17):11,487–11,490, 1993.
- [134] B. Simon. Almost periodic Schrödinger operators: A review. *Adv. Appl. Math.*, 3:463, 1982.
- [135] Y. Sinai. Anderson localization for one-dimensional difference Schrödinger operators with quasi-periodic potentials. In M. Mebkhout and R. Seneor, editors, *VIIIth International Congress on Mathematical Physics*. World-Scientific, Singapore, 1987.
- [136] S. Smirnov. Critical percolation in the plane: conformal invariance, Cardy’s formula, scaling limits. *C. R. Acad. Sci. Paris Sér. I Math.*, 333(3):239–244, 2001.
- [137] D. Stauffer and A. Aharony. *Introduction to Percolation Theory, Second Edition*. Taylor and Francis Ltd., London, 1992.
- [138] K. R. Steffen, Y. Epshteyn, J. Zhu, J. W. Deming, and K. M. Golden. Network modeling of fluid transport through sea ice with entrained exopolymeric substances. 9 pp., Preprint, 2016.
- [139] A. D. Stone, P. A. Mello, K. A. Muttalib, and J. L. Pichard. *Random Matrix Theory and Maximum Entropy Models for Disordered Conductors*, chapter 9, pages 369–448. Elsevier Science Publishers, Amsterdam, Netherlands, 1991.
- [140] M. H. Stone. *Linear Transformations in Hilbert Space*. American Mathematical Society, Providence, RI, 1964.
- [141] C. Strong. Atmospheric influence on Arctic marginal ice zone position and width in the Atlantic sector, February–April 1979–2010. *Climate Dynamics*, 39(12):3091–3102, 2012.

- [142] C. Strong, D. Foster, E. Cherkaev, I. Eisenman, and K. M. Golden. On the definition and analysis of the width of the marginal ice zone. *Journal of Atmospheric and Oceanic Technology*, under review, 2016.
- [143] C. Strong and K. M. Golden. Filling the polar data gap in sea ice concentration fields using partial differential equations. *Remote Sensing*, 8(6):442–451, invited, 2016.
- [144] C. Strong and I. G. Rigor. Arctic marginal ice zone trending wider in summer and narrower in winter. *Geophys. Res. Lett.*, 40(18), 2013.
- [145] I. A. Sudakov, S. A. Vakulenko, and K. M. Golden. Arctic melt ponds and bifurcations in the climate system. *Comm. Nonlinear Science and Numerical Simulation*, 22(1-3):70–81, 2015.
- [146] T. Tao and V. Vu. Random matrices: Universality of local eigenvalue statistics up to the edge. *Communications in Mathematical Physics*, 298(2):549–572, 2010.
- [147] C. J. Thompson. *Classical Equilibrium Statistical Mechanics*. Oxford University Press, Oxford, 1988.
- [148] S. Torquato. *Random Heterogeneous Materials: Microstructure and Macroscopic Properties*. Springer-Verlag, New York, 2002.
- [149] C.A. Tracy and H. Widom. Fredholm determinants, differential equations and matrix models. *Comm. Math. Phys.*, 163(1):33–72, 1994.
- [150] C.A. Tracy and H. Widom. Level-spacing distributions and the Airy kernel. *Comm. Math. Phys.*, 159(1):151–174, 1994.
- [151] B. Tsirelson and W. Werner. *Lectures on probability theory and statistics*, volume 1840 of *Lecture Notes in Mathematics*. Springer-Verlag, Berlin, 2004. Lectures from the 32nd Probability Summer School held in Saint-Flour, July 7–24, 2002, Edited by Jean Picard.
- [152] A.M. Tulino and S. Verdú. Random matrix theory and wireless communications. *Commun. Inf. Theory*, 1(1):1–182, June 2004.
- [153] G. Wainrib and J. Touboul. Topological and dynamical complexity of random neural networks. *Phys. Rev. Lett.*, 110:118101, Mar 2013.
- [154] E. P. Wigner. On the distribution of the roots of certain symmetric matrices. *Ann. Math.*, 67(2):325–327, 1958.
- [155] M. Wright and R. Weaver. *New Directions in Linear Acoustics and Vibration: Quantum Chaos, Random Matrix Theory and Complexity*. Cambridge University Press, 2010.
- [156] J. Xin. *An Introduction to Fronts in Random Media*. Surveys and Tutorials in the Applied Mathematical Sciences. Springer New York, 2009.
- [157] F. Zhou, B. Spivak, N. Taniguchi, and B. L. Altshuler. Giant microwave absorption in metallic grains: Relaxation mechanism. *Phys. Rev. Lett.*, 77(10):1958–1961, 1996.
- [158] J. Zhu, K. M. Golden, A. Gully, and C. Sampson. A network model for electrical transport in sea ice. *Physica B (Condensed Matter)*, 405(14-15):3033–3036, 2010.
- [159] J. Zhu, A. Jabini, K. M. Golden, H. Eicken, and M. Morris. A network model for fluid transport in sea ice. *Ann. Glaciol.*, 44:129–133, 2006.

Budget Justification

Salary: The bulk of the funds being requested are to support the participants in the project. In particular, we are requesting 1 month salary each for: the PI Golden and the Co-PI's Cherkaev and Alberts. We are requesting partial support for one Ph.D. student in the Department of Mathematics (\$22,826 each academic year), and support for one undergraduate student (\$5,000 total each academic year). Salary support in years two and three assumes 3% annual pay increase for senior personnel.

Travel: Requests for travel funding are to support the participants in presenting our results at conferences, such as the SIAM Annual Meeting, the Fall American Geophysical Union (AGU) Meeting, and meeting specifically on random matrix theory. Funding is requested for three domestic and two international trips each year. This portion of the funding will also support visitors working in closely related areas, or trips by the PI and co-PI's to visit colleagues working on closely related problems.

Publications: \$2000 per year is requested for publications in journals with page charges or flat fees.

Materials and supplies: \$3,000 annually for technical supplies including software licenses, computer hardware, and data storage units.

Consultant services: \$8,000 annually to compensate N. Benjamin Murphy for his contributions to the proposed research. Dr. Murphy is an expert on the analytic continuation method, the computation of spectral measures, and the effective behavior of the advection diffusion equation. He is lead author on the key paper that led to the discoveries on which this grant is based.

Indirect costs: The current Indirect Cost rate at the University of Utah is 51%. It will be 51.5% next year, and 52.5% in subsequent years.